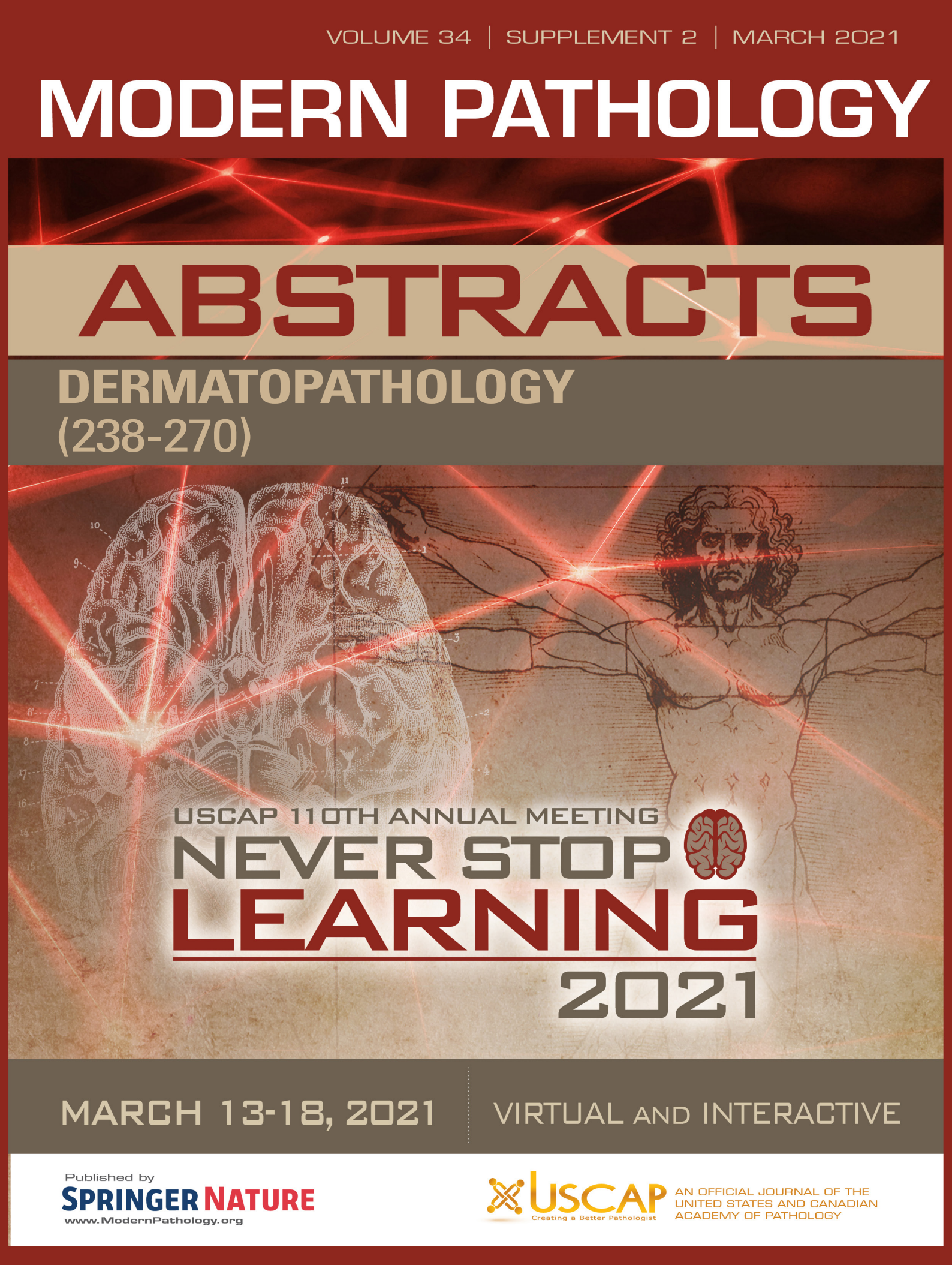


# MODERN PATHOLOGY

## ABSTRACTS

AUTOPSY AND FORENSICS  
(1-32)



USCAP 110TH ANNUAL MEETING  
**NEVER STOP**  
**LEARNING**  
**2021**

MARCH 13-18, 2021

VIRTUAL AND INTERACTIVE

Published by  
**SPRINGER NATURE**  
[www.ModernPathology.org](http://www.ModernPathology.org)

 **USCAP** AN OFFICIAL JOURNAL OF THE  
UNITED STATES AND CANADIAN  
ACADEMY OF PATHOLOGY  
Creating a Better Pathologist

EDUCATION COMMITTEE

Jason L. Hornick  
Chair

Rhonda K. Yantiss, Chair  
Abstract Review Board and Assignment Committee

Kristin C. Jensen  
Chair, CME Subcommittee

Laura C. Collins

Interactive Microscopy Subcommittee

Raja R. Seethala  
Short Course Coordinator

Ilan Weinreb  
Subcommittee for Unique Live Course Offerings

David B. Kaminsky  
(Ex-Officio)  
Zubair W. Baloch  
Daniel J. Brat  
Sarah M. Dry  
William C. Faquin  
Yuri Fedoriw  
Karen Fritchie  
Jennifer B. Gordetsky  
Melinda Lerwill  
Anna Marie Mulligan

Liron Pantanowitz  
David Papke,  
Pathologist-in-Training  
Carlos Parra-Herran  
Rajiv M. Patel  
Deepa T. Patil  
Charles Matthew Quick  
Lynette M. Sholl  
Olga K. Weinberg  
Maria Westerhoff  
Nicholas A. Zoumberos,  
Pathologist-in-Training

ABSTRACT REVIEW BOARD

Benjamin Adam  
Rouba Ali-Fehmi  
Daniela Allende  
Ghassan Allo  
Isabel Alvarado-Cabrero  
Catalina Amador  
Tatjana Antic  
Roberto Barrios  
Rohit Bhargava  
Luiz Blanco  
Jennifer Boland  
Alain Borczuk  
Elena Brachtel  
Marilyn Bui  
Eric Burks  
Shelley Caltharp  
Wenqing (Wendy) Cao  
Barbara Centeno  
Joanna Chan  
Jennifer Chapman  
Yunn-Yi Chen  
Hui Chen  
Wei Chen  
Sarah Chiang  
Nicole Cipriani  
Beth Clark  
Alejandro Contreras  
Claudiu Cotta  
Jennifer Cotter  
Sonika Dahiya  
Farbod Darvishian  
Jessica Davis  
Heather Dawson  
Elizabeth Demicco  
Katie Dennis  
Anand Dighe  
Suzanne Dintzis  
Michelle Downes

Charles Eberhart  
Andrew Evans  
Julie Fanburg-Smith  
Michael Feely  
Dennis Firchau  
Gregory Fishbein  
Andrew Folpe  
Larissa Furtado  
Billie Fyfe-Kirschner  
Giovanna Giannico  
Christopher Giffith  
Anthony Gill  
Paula Ginter  
Tamar Giorgadze  
Purva Gopal  
Abha Goyal  
Rondell Graham  
Alejandro Gru  
Nilesh Gupta  
Mamta Gupta  
Gillian Hale  
Suntrea Hammer  
Malini Harigopal  
Douglas Hartman  
Kammi Henriksen  
John Higgins  
Mai Hoang  
Aaron Huber  
Doina Ivan  
Wei Jiang  
Vickie Jo  
Dan Jones  
Kirk Jones  
Neerja Kambham  
Dipti Karamchandani  
Nora Katabi  
Darcy Kerr  
Francesca Khani

Joseph Khoury  
Rebecca King  
Veronica Klepeis  
Christian Kunder  
Steven Lagana  
Keith Lai  
Michael Lee  
Cheng-Han Lee  
Madelyn Lew  
Faqian Li  
Ying Li  
Haiyan Liu  
Xiuli Liu  
Lesley Lomo  
Tamara Lotan  
Sebastian Lucas  
Anthony Magliocco  
Kruti Maniar  
Brock Martin  
Emily Mason  
David McClintock  
Anne Mills  
Richard Mitchell  
Neda Moatamed  
Sara Monaco  
Atis Muehlenbachs  
Bita Naini  
Dianna Ng  
Tony Ng  
Michiya Nishino  
Scott Owens  
Jacqueline Parai  
Avani Pendse  
Peter Pytel  
Stephen Raab  
Stanley Radio  
Emad Rakha  
Robyn Reed

Michelle Reid  
Natasha Rekhman  
Jordan Reynolds  
Andres Roma  
Lisa Rooper  
Avi Rosenberg  
Esther (Diana) Rossi  
Souzan Sanati  
Gabriel Sica  
Alexa Siddon  
Deepika Sirohi  
Kalliopi Siziopikou  
Maxwell Smith  
Adrian Suarez  
Sara Szabo  
Julie Teruya-Feldstein  
Khin Thway  
Rashmi Tondon  
Jose Torrealba  
Gary Tozbikian  
Andrew Turk  
Evi Vakiani  
Christopher VandenBussche  
Paul VanderLaan  
Hannah Wen  
Sara Wobker  
Kristy Wolniak  
Shaofeng Yan  
Huihui Ye  
Yunshin Yeh  
Anjana Yeldandi  
Gloria Young  
Lei Zhao  
Minghao Zhong  
Yaolin Zhou  
Hongfa Zhu

To cite abstracts in this publication, please use the following format: **Author A, Author B, Author C, et al. Abstract title (abs#). In "File Title." *Modern Pathology* 2021; 34 (suppl 2): page#**

**1 Hepatosplenic T-CELL Lymphoma Found on Autopsy in an Acutely Ill Patient who Presented with Right Upper Quadrant Pain**

Syed Abbas<sup>1</sup>, Maryam Aghighi<sup>1</sup>, Pooja Devi<sup>2</sup>, Jonathan Harris<sup>1</sup>

<sup>1</sup>Saint Barnabas Medical Center/RWJBarnabas Health, Livingston, NJ, <sup>2</sup>Saint Barnabas Medical Center, Livingston, NJ

**Disclosures:** Syed Abbas: None; Maryam Aghighi: None; Pooja Devi: None; Jonathan Harris: None

**Background:** Hepatosplenic T-cell lymphoma (HSTL) is a systemic extranodal malignancy of cytotoxic T-cells comprising of 1% of all peripheral T-cell lymphomas. Patients typically present with systemic symptoms, hepatomegaly, and splenomegaly. Histopathologically, the cells of HSTL are monotonous, with medium-sized nuclei and a rim of pale cytoplasm that manifest with marked sinusoidal infiltration of the liver, spleen, and bone marrow. The clinical course is aggressive and early use of high dose chemotherapy with subsequent hematopoietic stem cell transplantation may improve survival.

**Design:** A 51-year-old female presented to the emergency room with complaints of shortness of breath, dizziness, and right upper quadrant pain. A general physical examination was significant for jaundice and decreased breath sounds in both lungs. Imaging studies were done which revealed consolidation of lungs, mild hepatomegaly and thickening of the gallbladder. Laboratory tests revealed elevated LFT's. ERCP was performed to find out a possible cause of jaundice. Thickening of the gallbladder was noted and no stones were found. Patient was diagnosed to have acalculous cholecystitis and a decision was made to do a laparoscopic cholecystectomy. During the laparoscopic procedure, an enlarged liver with multiple areas of hemorrhage was seen. Soon after the operation, patient became febrile and hypotensive. Patient was then transferred to ICU, where she lost pulse and was given advanced cardiac life support. However, it was not successful, and the patient was pronounced dead.

**Results:** Autopsy revealed gross findings of an enlarged liver with marked hemorrhage and necrosis. Laboratory results revealed elevated liver function tests, pancytopenia, and significantly high ferritin. Coagulation abnormalities included elevated prothrombin time, elevated partial thromboplastin time and low platelet count. Sections from the liver showed neoplastic lymphocytes within liver sinusoids (Figure 1). Immunohistochemical stains showed the neoplastic cells were positive for CD3, CD2, CD7 and CD56 and negative for CD5, CD4, and CD8. Ki-67 was variable with focal areas up to 40%. Spleen was also involved where expansion of the red pulp was seen with cords infiltrated by numerous intermediate sized lymphoid cells (Figure 2).

Figure 1 - 1

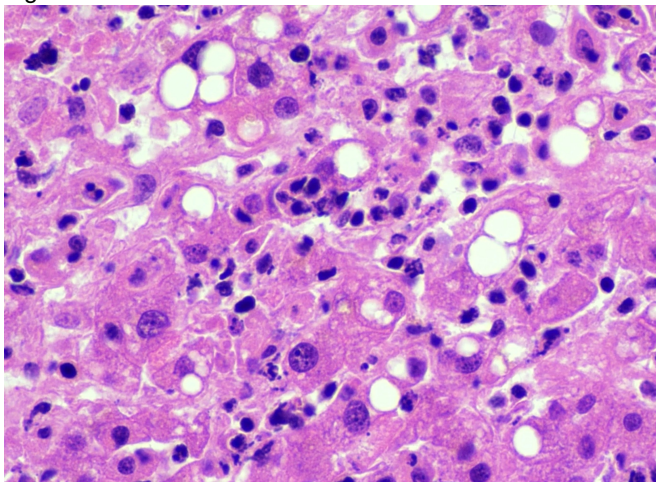
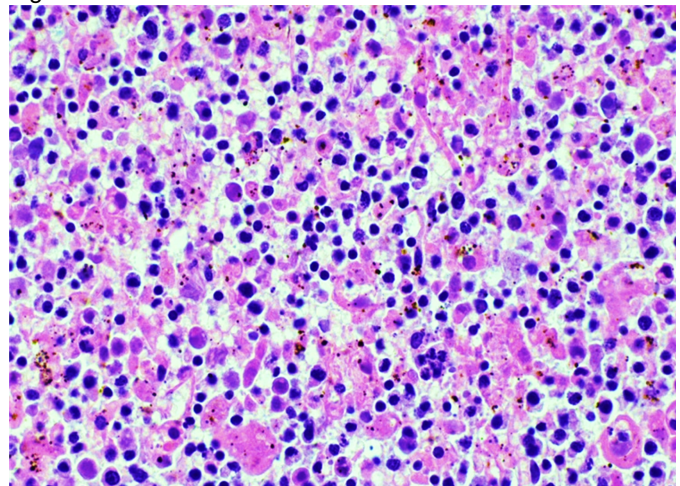


Figure 2 - 1



**Conclusions:** HSTL is an aggressive extranodal T-cell lymphoma that affects the liver, spleen, and bone marrow. Patients usually present with systemic symptoms, hepatosplenomegaly and aberrant lab results including abnormal liver function tests, coagulation abnormalities and anemia with often leukopenia and thrombocytopenia. In the current case, patient's liver, spleen, and bone marrow were involved by neoplastic T cells and she had multiple areas of hepatic hemorrhage due to coagulation abnormalities. The coagulative abnormalities are indicative of a picture of DIC that eventually led to the patient's demise.

## 2 Intra-Abdominal Hemorrhage Secondary to Gallbladder Perforation

Maryam Aghighi<sup>1</sup>, Dionnee James<sup>1</sup>, Jonathan Harris<sup>1</sup>

<sup>1</sup>Saint Barnabas Medical Center/RWJBarnabas Health, Livingston, NJ

**Disclosures:** Maryam Aghighi: None; Dionnee James: None; Jonathan Harris: None

**Background:** Hemorrhagic cholecystitis in combination with gallbladder perforation is a rare complication of acute cholecystitis and is associated with a high mortality rate. Early detection is a challenge as the clinical presentation mimics that of acute cholecystitis. With very few reported cases in the literature, we present an autopsy case of a patient with intra-abdominal hemorrhage due to gallbladder perforation.

**Design:** The patient was a 56-year-old male who presented to the emergency department with complaints of abdominal pain and nausea. The abdominal pain was mostly present in the epigastric region with some radiation to the back. Labs initially showed increased total bilirubin, elevated AST, ALP, and lipase. An ultrasound of the abdomen showed cholelithiasis with gallbladder sludge, splenomegaly and a small amount of right upper quadrant ascites. MRCP was also performed and showed a possible mass involving the gallbladder and adjacent inferior soft tissues. Shortly following MRCP, he developed a seizure, hypotension and tachycardia with worsening liver functions, lactic acidosis, hyperammonemia, elevated troponin I, decreased hemoglobin and increased WBC with bandemia. Coagulation studies showed increased PT and INR. Treatment with vasopressors proved futile. His status was changed to DNR, and the patient was pronounced dead.

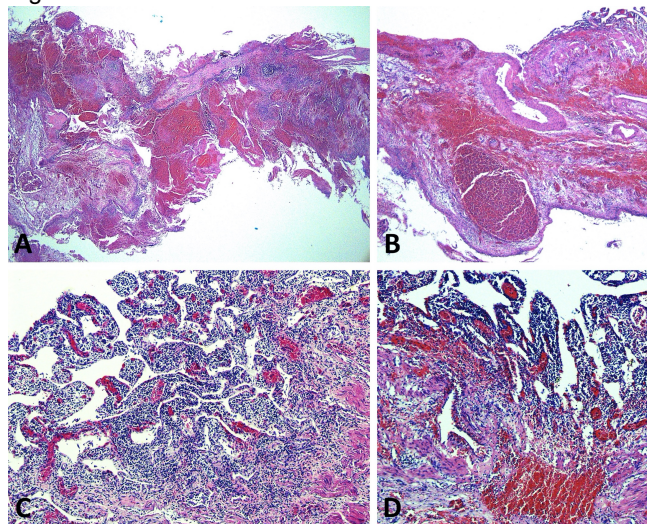
**Results:** Postmortem examination revealed 2.5 liter of blood in the peritoneal cavity, free wall perforation of the gallbladder, severe hepatic cirrhosis and splenomegaly. Histologic examination revealed a gallbladder with extensive hemorrhagic changes and acute and chronic inflammation.

Figure 1 - 2



**Figure 1-** Gross specimen showing gallbladder with transmurial defect (2.5 × 0.5 cm) with hemorrhagic serosa

Figure 2 - 2



**Figure 2-** A and B: Gallbladder with hemorrhage and free wall perforation (H&E, ×20) and C and D: Gallbladder with acute and chronic cholecystitis (H&E, ×100)

**Conclusions:** Hemorrhagic cholecystitis and gallbladder perforation are uncommon complications of acute cholecystitis and associated with high mortality rates. Inflammation of the gallbladder wall, mucosal necrosis and ulceration may lead to hemorrhagic cholecystitis. It is suggested that perforation in cases of hemorrhagic cholecystitis is due to elevated intraluminal pressure in the presence of predisposing factors such as bleeding diathesis, trauma, malignancy or anticoagulation therapy which cause bleeding inside the gallbladder. In literature, most reported cases of intra-abdominal hemorrhage are secondary to gallbladder transhepatic perforation with even fewer cases of free wall rupture.

Bleeding in the setting of hypocoagulability contributed to massive intra-abdominal hemorrhage secondary to gallbladder perforation, which was determined to be the cause of death in this case.

### **3 Improving Autopsy Correct Consent Rates through Interdisciplinary Communication: An Unforeseen Outcome of the COVID-19 Pandemic**

Abigail Alexander<sup>1</sup>, Katelyn Dannheim<sup>2</sup>

<sup>1</sup>Brown University Lifespan Academic Medical Center, Providence, RI, <sup>2</sup>Rhode Island and Hasbro Children's Hospitals, Providence, RI

**Disclosures:** Abigail Alexander: None; Katelyn Dannheim: *Consultant*, K.D. has received consulting fees from PathAI for work unrelated to this manuscript

**Background:** Autopsy rates have been steadily declining since the Joint Commission on the Accreditation of Hospitals abolished minimum autopsy requirements, citing exorbitant costs, the onerous process of obtaining consent, and the erroneous belief that autopsies were becoming irrelevant in the era of advance imaging. However, studies have suggested that as many as 24% of autopsy cases identify a major diagnosis unknown by clinicians at the time of death for which treatment would have changed the outcome. Autopsies remain a fundamental part of medical education and quality improvement, though the logistics of consent continue to be burdensome. At this institution, the autopsy service suffered from frequent errors in consent. A quality improvement analysis from July 2019 to February 2020 found that 60% of autopsy consent forms contained an error. The average time to obtaining a corrected consent was 7 hours and 39 minutes. Delays such as this are not uncommon in autopsy pathology services and may result in the unintended consequences of tissue degradation and postponement of postmortem services for the deceased.

**Design:** Due to the COVID-19 pandemic, increased communication between the clinical and autopsy pathology teams was recommended in an attempt to provide clear and consistent guidance regarding postmortem examination and to reduce risk. Clinicians were asked to page the on-call autopsy resident for each new autopsy request and an autopsy consent guide was implemented to help pathology residents with the new process. Consent error rates in July through September were compared in 2019 and 2020.

**Results:** The autopsy consent error rate decreased from 56% to 26% ( $p=0.02$ ), while the rate of overall autopsies increased by 36% in July-September 2020 compared to 2019. The average time to obtain corrected consent forms did not significantly change.

**Conclusions:** Interdepartmental communication and implementation of the "autopsy consent guide" significantly decreased the consent error rate while introducing a framework of how to deal with the increased risks associated with the COVID-19 pandemic for all stakeholders involved. Interestingly, the average time needed to correct an error did not significantly change, suggesting that once an error occurs there are likely factors at play beyond the scope of this intervention. Further investigation is needed to fully understand the complexities of the consent process contributing to errors and delays.

### **4 Assessment of Racial Inequities in Recent US Pediatric Autopsy Rates**

Abigail Alexander<sup>1</sup>, Sonja Chen<sup>2</sup>, Sarah Andrea<sup>2</sup>, Katelyn Dannheim<sup>3</sup>

<sup>1</sup>Brown University Lifespan Academic Medical Center, Providence, RI, <sup>2</sup>Rhode Island Hospital, Providence, RI, <sup>3</sup>Rhode Island and Hasbro Children's Hospitals, Providence, RI

**Disclosures:** Abigail Alexander: None; Sonja Chen: None; Sarah Andrea: None; Katelyn Dannheim: None

**Background:** Due in part to diagnostic improvements and financial, legal, and administrative disincentives, clinical autopsy rates in the US have declined substantially since the 1990s. However, improvements in diagnostic medicine and health care are not equitably distributed. A recent study in adults found autopsy rates were highest for Black decedents across multiple natural causes of death. It is also known that there are striking differences in infant and child mortality across race and ethnicity. We examined the association between race, autopsy status, and cause of death in US pediatric decedents.

**Design:** Using Centers for Disease Control and Prevention, National Center for Health Statistics Multiple Cause of Death data from 2004-2018, we examined mortality rate and proportion autopsied by race/ethnicity, age, and cause of death for all non-forensic decedents 0-24 years of age. Cause of death (treatable, preventable, non-preventable and non-treatable, or unknown) was defined using the Office for National Statistics Revised Definition

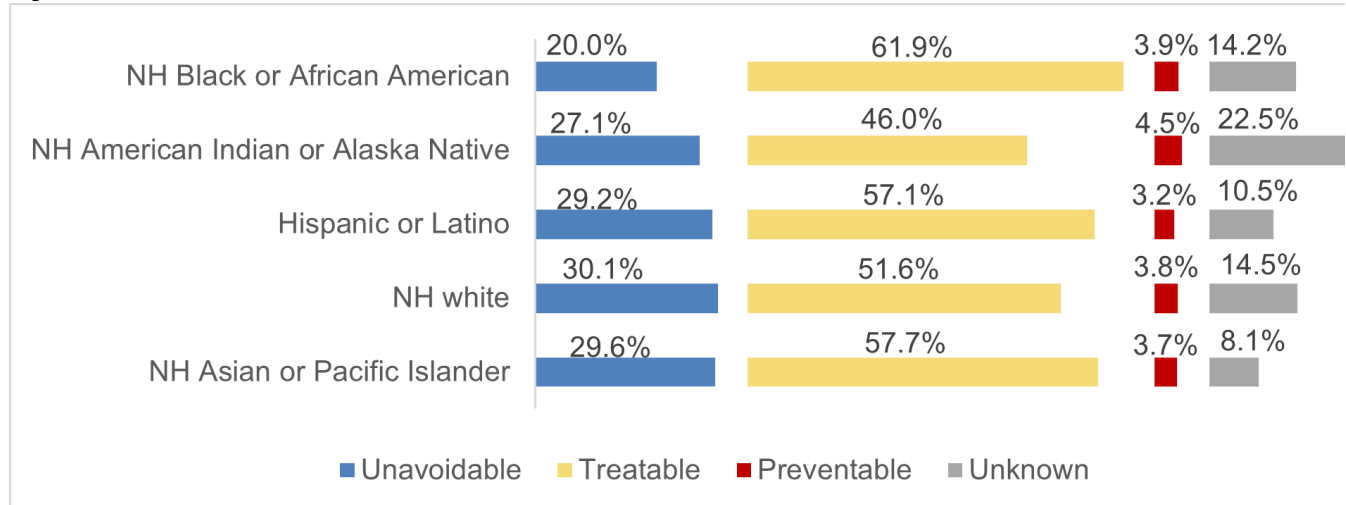
of Avoidable Mortality. Using log-linear Poisson generalized linear models, we modeled autopsy status as a function of race/ethnicity and age.

**Results:** Overall, 29% of the 452,225 non-forensic pediatric decedents underwent an autopsy. Relative to white children, deceased non-Hispanic (NH) Black children and NH American Indian or Alaskan Native children were more likely to undergo an autopsy while Hispanic and NH Asian children were less likely (Table 1). For NH Black children, this finding persisted across all age groups, particularly in the 5 to 10-year age group (36% of NH Black vs. 22.6 of NH white; Relative Risk: 1.61 [95% Confidence Interval:1.52,1.70]). Relative to white children, disproportionately more of the deaths among NH Black and NH American Indian or Alaska Native children were due to treatable conditions (such as asthma) or unknown causes, respectively (Figure 1).

Age Group	Measure	Race/Ethnicity				
		Non-Hispanic white	Non-Hispanic Black or African American	Non-Hispanic American Indian or Alaska Native	Non-Hispanic Asian or Pacific Islander	Hispanic
0-24	Proportion Autopsied	29.6	31.4	36.1	21.8	25.6
	RR (95% CI)*	Referent	<b>1.10 (1.09,1.11)</b>	<b>1.16 (1.13,1.21)</b>	<b>0.72 (0.70,0.74)</b>	<b>0.83 (0.82,0.84)</b>
< 1 year	Proportion Autopsied	27.6	28.0	35.5	19.2	23.1
	RR (95% CI)	Referent	<b>1.04 (1.02,1.04)</b>	<b>1.22 (1.17,1.28)</b>	<b>0.67 (0.65,0.70)</b>	<b>0.79 (0.77,0.80)</b>
1 to 4 years	Proportion Autopsied	38.3	49.5	46.8	30.4	35.2
	RR (95% CI)	Referent	<b>1.28 (1.24,1.33)</b>	<b>1.17 (1.05,1.31)</b>	<b>0.77 (0.70,0.85)</b>	<b>0.88 (0.84,0.92)</b>
5 to 10 years	Proportion Autopsied	22.6	36.0	22.2	23.0	23.8
	RR (95% CI)	Referent	<b>1.61 (1.52,1.70)</b>	0.94 (0.72,1.21)	1.00 (0.88,1.14)	1.00 (0.94,1.08)
11 to 17 years	Proportion Autopsied	29.0	42.6	31.9	24.3	28.8
	RR (95% CI)	Referent	<b>1.47 (1.42,1.53)</b>	1.04 (0.88,1.23)	<b>0.80 (0.72,0.90)</b>	<b>0.94 (0.90,0.99)</b>
18 to 24 years	Proportion Autopsied	37.7	40.8	39.5	30.0	36.2
	RR (95% CI)	Referent	<b>1.09 (1.06,1.11)</b>	1.01 (0.92,1.10)	<b>0.77 (0.72,0.83)</b>	<b>0.91 (0.89,0.94)</b>

\*Age-adjusted; Bolded red denoted significantly greater risk of autopsy and bolded blue denotes significantly lower risk of autopsy

Figure 1 - 4



**Conclusions:** Both autopsies and deaths due to treatable, preventable (such as diabetes mellitus), and/or unknown causes were more common for NH Black and American Indian or Alaska Native children highlighting persistent inequities in access to timely and quality care. While patient race/ethnicity affects clinical care and treatment, our study illustrates its effect on the postmortem investigation, suggesting that racial bias continues to play a role in healthcare even after death.

**5 A Sticky Issue: Thrombotic Phenomena Amidst Autopsy Findings in Fatal Cases of COVID-19**

Ahmad Alshomrani<sup>1</sup>, Joseph Rohr<sup>1</sup>, Matthew Carda<sup>1</sup>, Benjamin Swanson<sup>1</sup>, Kirk Foster<sup>1</sup>, Archana Kanteti<sup>1</sup>, Ashley Hein<sup>1</sup>, Stanley Radio<sup>1</sup>

<sup>1</sup>University of Nebraska Medical Center, Omaha, NE

**Disclosures:** Ahmad Alshomrani: None; Joseph Rohr: None; Matthew Carda: None; Benjamin Swanson: None; Kirk Foster: None; Archana Kanteti: None; Ashley Hein: None; Stanley Radio: None

**Background:** Coronavirus disease 2019, or COVID-19, is caused by the novel coronavirus SARS-CoV-2. Morbid risk factors include age, chronic conditions, male gender, obesity, altered coagulation, and substance use, among others. We characterized pre-mortem clinical findings in our patients with fatal COVID-19 with the autopsy findings in visceral organs and, for select patients, the GI tract.

**Design:** Post-mortem examinations were done on 9 patients who died with known antemortem COVID at our institution from February to September, 2020. Clinical and laboratory data were reviewed. Tissue examination was performed by light microscopy with routine H&E, and in selected blocks, histologic stains as well as immunohistochemical staining were performed by standard methods.

**Results:** The median age of our cohort was 67 years (range 35-85) and included 8/9 males. Clinical morbidities included hypertension (7/9), hyperlipidemia (5/9), diabetes (4/9), substance use (5/9), and BMI >30 (5/9). Pre-mortem laboratory findings included elevated D-dimer (4/9 tested) and elevated PTT (3/6 tested) but platelet counts were within reference range in 9/9. Pulmonary findings: diffuse alveolar damage, exudative (2/9) or proliferative (7/9) phases; acute bronchopneumonia (2/9); lymphocytic pneumonia (1/9); large vessel thrombi (3/9) and small vessel thrombi (7/9). Cardiac findings: cardiomegaly (6/9), coronary artery disease of 51-75% occlusion (8/9), healed ischemic disease (3/9); and acute myocardial infarction (2/9). Renal findings: acute tubular injury (7/9); large vessel thrombus (1/9), microthrombi (3/9); glomerulopathy (2/9); arteriosclerosis (3/9). GI findings: hepatic steatosis (4/9) hepatic centrilobular congestion (6/9); and ischemic bowel with associated microthrombi (1/9).

**Conclusions:** Pulmonary findings including DAD and pneumonia predominated and were usually accompanied by micro- and macrovascular thrombi. Cardiac findings included pre-existing cardiomegaly or CAD. However, in two

patients, acute myocardial infarct contributed to the immediate cause of death. Thrombi of varying degrees of occlusion were present in epicardial coronary arteries as well as small to medium intramural vessels and likely contributed to cardiac dysfunction. Significant myocardial inflammation was seen in 2/9 patients without myocyte necrosis. Acute tubular injury and centrilobular liver necrosis were common but likely secondary effects of septic hypotension.

## **6 SARS-CoV-2 S Gene Detection in Lung Tissue: A Retrospective Autopsy Study**

Diana Berman<sup>1</sup>, Alain Borczuk<sup>2</sup>, Steven Salvatore<sup>3</sup>, Hanna Rennert<sup>2</sup>, Phyllis Ruggiero<sup>4</sup>

<sup>1</sup>New York-Presbyterian/Weill Cornell Medical Center, New York, NY, <sup>2</sup>Weill Cornell Medicine, New York, NY, <sup>3</sup>Weill Cornell Medical Center, New York, NY <sup>4</sup>New York-Presbyterian Hospital, New York, NY

**Disclosures:** Diana Berman: None; Alain Borczuk: None; Steven Salvatore: None; Hanna Rennert: None; Phyllis Ruggiero: None

**Background:** Covid-19, caused by SARS-CoV-2, has been implicated as the cause of death in over 225,000 Americans as of 10/28/2020 since its emergence. We performed autopsies in whom no pre-mortem COVID-19 test was performed, prior to March 19, the date of the first nasopharyngeal (NP) swab confirmed positive autopsy at our institution. In retrospect, there were cases with clinical or autopsy findings suggestive of Covid-19. The goal of this study was to combine immunohistochemistry (IHC) and in situ hybridization (ISH) in lung tissue to validate a molecular test by RT-PCR on formalin-fixed paraffin embedded tissue (FFPE); this molecular test could then be applied to detect SARS-CoV-2 in lung tissue of previously untested cases.

**Design:** FFPE lung tissue sections from 51 autopsy cases were analyzed in two stages using a train-test design. In the first stage, we determined the test characteristics by comparing molecular results to testing by IHC and ISH using 19 positive controls with positive RT-PCR by NP swab and 11 negative controls from 2019. IHC was used to identify the SARS-CoV-2 viral spike protein (Genetex clone 1A9 at 1:75 dilution with 20-min antigen retrieval at pH 9.0 on Leica Bond III automated instrument) and positive sections were confirmed with ISH using RNAscope® technology (Advanced Cell Diagnostic) with probe pairs targeting the SARS-CoV-2 spike mRNA. All tissue blocks underwent viral RNA extraction by ThermoFisher and RT-PCR detection of SARS-CoV-2 with dual-target reagents (Altona Diagnostics) and the Rotor-Gene Q (Qiagen) thermal cycler. In the second stage, we tested an experimental cohort made up of consecutive autopsies done between January and March 19 and untested clinically suspicious cases using RT-PCR to detect the presence of SARS-CoV-2 in lung.

**Results:** In the first stage, IHC for spike protein and ISH for spike mRNA were positive in lung of 15 cases. In sections from those same blocks, RT-PCR detected the presence of the S gene in 13 cases. RT-PCR was negative in all 15 of the tissues negative by IHC with a sensitivity of 87%, specificity of 100%, positive predictive value of 100% and negative predictive value of 88%. In the second stage, 1 of 21 previously untested cases were positive for the S gene representing one case with consistent autopsy findings.

**Conclusions:** Molecular testing on FFPE tissue blocks is a sensitive and highly specific method to detect SARS-CoV-2 in lung tissue.

## **7 STAT6 Expression in the Lungs of Patients with COVID-19, an Autopsy Study**

Weibiao Cao<sup>1</sup>, Sonja Chen<sup>1</sup>, Mark Birkenbach<sup>2</sup>

<sup>1</sup>Rhode Island Hospital, Providence, RI, <sup>2</sup>Brown University, Rhode Island Hospital, Lifespan, Providence, RI

**Disclosures:** Weibiao Cao: None; Sonja Chen: None; Mark Birkenbach: None

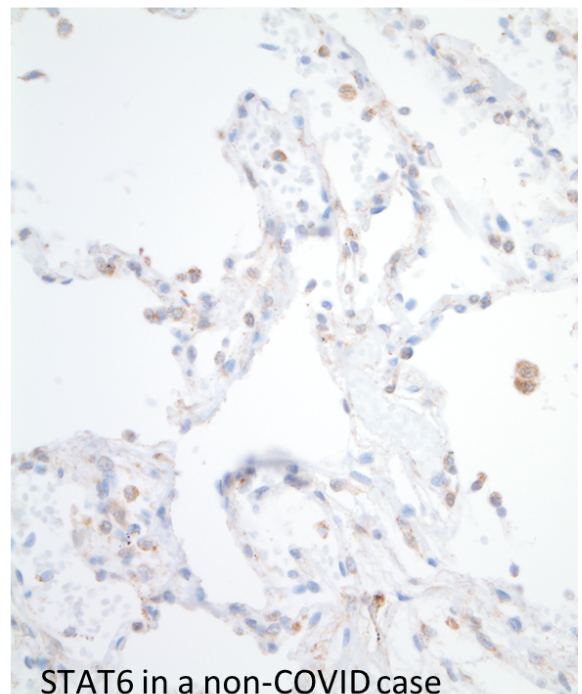
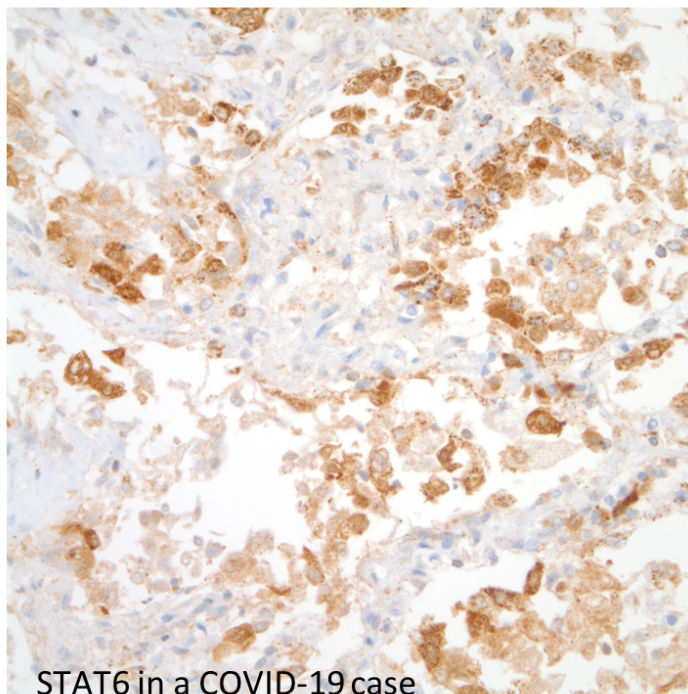
**Background:** Coronavirus disease 2019 (COVID-19) is caused by severe acute respiratory syndrome coronavirus 2 (SARS-CoV-2). Some COVID-19 patients suffer acute respiratory distress syndrome (ARDS), which may depend on a cytokine storm. Signal transducer and activator of transcription (STAT) 6 is a critical mediator of cytokine signaling. In this study we examined the expression of STAT6 in the lungs from patients with COVID-19.



**Design:** Autopsies were performed in six COVID-19 patients in 2020. Six control autopsy cases were also included from the same period. Immunostaining for STAT6, CD3, CD4, CD8, CD68 and broad-spectrum keratins was performed. The number of pneumocytes, macrophages, CD3+, CD4+ and CD8+ lymphocytes was counted

**Results:** The average age of six COVID-19 patients was  $60.8 \pm 4.9$ , including four females and two males. The disease duration was 7-57 days (average  $21.7 \pm 7.5$ ). The comorbidity in COVID-19 patients included hypertension (6/6), diabetes (4/6), sickle cell disease (1/6), end-stage kidney disease (1/6) and obesity (1/6). The average age of the control patients was  $63 \pm 6.9$ , which was not significantly different from the COVID group. The weight of bilateral lungs had no significant difference between COVID-19 and control. The number of pneumocytes, macrophages, CD3+, CD4+ and CD8+ lymphocytes per high power field was significantly increased in COVID-19 patients when compared with control ( $245 \pm 41.9$  vs  $86.2 \pm 19.7$  ( $P < 0.01$ ),  $153.8 \pm 25.2$  vs  $56.7 \pm 9.3$  ( $P < 0.01$ ),  $125 \pm 7.6$  vs  $56.7 \pm 15.4$  ( $P < 0.01$ ),  $48.5 \pm 8.7$  vs  $16.8 \pm 4.3$  ( $P < 0.01$ ) and  $46.2 \pm 11.7$  vs  $14.2 \pm 4.9$  ( $P < 0.05$ )). There was no significant difference of CD8/CD4 ratio between COVID-19 and control ( $1.06 \pm 0.26$  vs  $0.94 \pm 0.27$ ). STAT6 immunostaining showed cytoplasmic staining and was significantly increased in pneumocytes (2-3+ in 6/6) and lymphocytes (2-3+ in 5/6) in patients with COVID-19. The staining intensity in endothelial cells and macrophages was 0-1+ and not significantly different between COVID-19 and control.

Figure 1 - 7



**Conclusions:** The number of pneumocytes, macrophages, CD3+, CD4+ and CD8+ lymphocytes was significantly increased in COVID-19 patients. STAT6 cytoplasmic staining was much stronger in pneumocytes and lymphocytes in COVID-19 than control. The data imply that STAT6 may be an important mediator during cytokine storm in patients with COVID-19.

**8 Disseminated Invasive Fungal Infection, a Retrospective Autopsy Study Over a 20-Year Period**

Weibiao Cao, Rhode Island Hospital, Providence, RI

**Disclosures:** Weibiao Cao: None

**Background:** Invasive fungal infection (IFI) is one of the causes of death in immunocompromised patients. With the advance of the technologies and antifungal treatments, whether the incidence of invasive fungal infection has changed over the time is not clear. In this study, we analyzed all invasive fungal infection autopsy cases over the past twenty years.

**Design:** A retrospective study of autopsies was performed on patients with invasive fungal infection at Rhode Island Hospital and The Miriam Hospital from 2000 to 2019. The pertinent clinical information was collected and the pathologic data were reviewed in detail.

**Results:** Among 1930 autopsy cases, 11 cases (0.6%) were found to have invasive fungal infection, including 7 males and 4 females. The average age at death for these 11 cases was 51.1 years (range 4-79 years). The incidence of IFI was 0.3% from 2000 to 2009 and 0.8% from 2010 to 2019. The difference of incidence was not statistically significant. Of 11 cases, invasive candidiasis (5/11, 45.4%), invasive mucormycosis (3/11, 27.3%) and invasive aspergillosis (3/11, 27.3%) were the most common ones. The others included *Scedosporium* (1/11, 9%) and *fusarium* (1/11, 9%). There were two cases with mixed infections (candidiasis plus mucormycosis or aspergillosis plus mucormycosis, 2/11, 18.2%). Hematological malignancies (7/11, 63.6%) were the most common underlying disease. Others included cirrhosis (2/11, 18.2%), carcinoma (1/11, 9%) and renal transplant (1/11, 9%). Most commonly involved organs were lungs (9/11, 81.8%), heart (9/11, 81.8%), kidneys (9/11, 81.8%), thyroid gland (7/11, 63.6%), brain (6/11, 54.5%), spleen (5/11, 45.5%), liver (4/11, 36.4%), lymph nodes (3/11, 27.3%) and GI tract (3/11, 27.3%). Majority of cases (9/11, 81.8%) had acute inflammation and abscess formation, whose WBCs were 0.3-46.5 x 10<sup>9</sup>/L (average 11 ± 4.9 x 10<sup>9</sup>/L). WBC counts of two cases without inflammatory response were <0.2 x 10<sup>9</sup>/L. Only two cases (2/11, 18.2%) showed focal necrotizing granulomas.

**Conclusions:** The incidence of IFI did not decrease in the past twenty years. The most common organisms of IFI were candida, mucor and aspergillus species. The most commonly involved organs were lungs, heart, kidneys, thyroid gland, brain and spleen. Majority of cases had acute inflammatory responses with rare cases having necrotizing granuloma.

**9 Fatal Intracerebral Hemorrhage in a COVID-19 Patient**

Garrett Chan<sup>1</sup>, John DeWitt<sup>2</sup>, Kirsten Threlkeld<sup>2</sup>

<sup>1</sup>Larner College of Medicine at the University of Vermont, Burlington, VT, <sup>2</sup>University of Vermont Medical Center, Burlington, VT

**Disclosures:** Garrett Chan: None

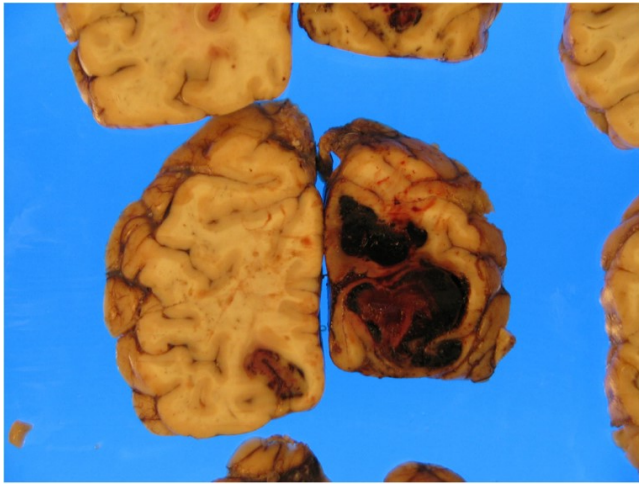
**Background:** Coronavirus disease 2019 (COVID-19) is primarily known to lead to respiratory illness, as the causative virus, SARS-CoV2, invades the respiratory epithelium. Accordingly, most patients with COVID-19 describe symptoms such as cough, shortness of breath, and fever; however, neurologic sequelae and symptoms have also been reported, including loss of olfactory sense, impaired mental acuity post-disease, and strokes. Reports on neurologic effects secondary to COVID-19 and their pathologic basis have been added to the literature, but our understanding remains incomplete. Here, we report the neuropathologic findings in a COVID-19 patient with fatal intracerebral hemorrhage.

**Design:** The patient was a 72-year-old man who presented to the University of Vermont Medical Center with signs of severe multiorgan dysfunction, including acute respiratory failure, elevated D-dimer, and episodes of hypotension. He went into acute hypoxic decline with severe decline in neurologic function. Consent from family was obtained and an autopsy was performed, which included examination of the brain.

**Results:** Gross examination during autopsy revealed multiple hemorrhagic infarcts in the right and left occipital lobes as well as a subacute hemorrhagic infarct in the right frontal lobe white matter. On microscopic examination,

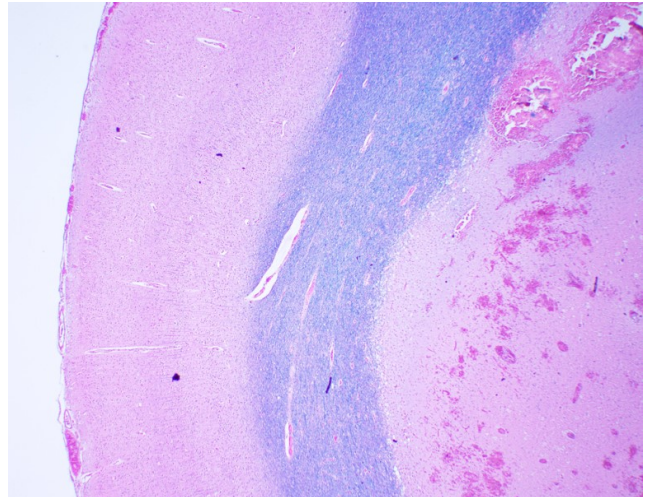
this frontal lobe infarct was significant for macrophages and swollen axons. In the right occipital lobe infarct, we identified blurring of the gray-white junction and hemorrhagic transformation. The right occipital lobe infarct featured myelin-laden macrophages and spongiotic change. Additionally, hemosiderin-laden macrophages and thickened, hyalinized arterial walls were noted in the cerebral arteries, suggesting arteriosclerosis. Lastly, Lewy bodies were identified in the locus ceruleus, consistent with early-stage Lewy Body disease.

Figure 1 - 9



10:01 0505 1qA 05 - E40-05UA

Figure 2 - 9



**Conclusions:** Our patient suffered from multiple infarcts, likely from a thrombotic or embolic source with subsequent hemorrhagic transformation. Changes in blood pressure during his hospital course may have contributed to reperfusion injury and hemorrhagic transformation, while the right frontal lobe lesion may represent the “acute disseminated encephalomyelitis (ADEM)-like” lesions described in the early COVID-19 neuropathologic literature. This case adds to the relatively scant literature of the associated neuropathologic sequelae of COVID-19 infection; however, further neuropathologic examinations of COVID-19 patients are needed to fully elucidate the pathophysiology by which inflammation and hemodynamic changes affect the brain.

**10 Pathological Features of SARS-CoV-2 Associated Myocardial Injury in COVID-19 Related Deaths: Report of 18 Cases**

Corey Chang<sup>1</sup>, Mercury Lin<sup>1</sup>, Eric Vail<sup>1</sup>, Warren Tourtellotte<sup>1</sup>, Siddharth Singh<sup>1</sup>, Daniel Luthringer<sup>2</sup>  
<sup>1</sup>Cedars-Sinai Medical Center, Los Angeles, CA, <sup>2</sup>Cedars-Sinai Medical Center, West Hollywood, CA

**Disclosures:** Corey Chang: None; Mercury Lin: None; Eric Vail: None; Warren Tourtellotte: None; Siddharth Singh: None; Daniel Luthringer: None

**Background:** Severe acute respiratory distress syndrome coronavirus 2 (SARS-CoV-2) is a highly infectious virus and cause of an ongoing pandemic with significant morbidity and mortality. Serious cardiovascular complications occur, with limited understanding of the pathophysiology. We studied hearts from autopsies of a cohort of patients who died of COVID-19 to provide a detailed report of cardiac pathology including histologic changes and molecular and ultrastructural evidence of SARS-CoV-2 virus within cardiac tissue.

**Design:** Autopsies from patients who died of COVID-19 at Cedars-Sinai Medical Center (Los Angeles, CA) were included. Clinical and laboratory data were reviewed. Hearts were examined for gross and microscopic features to identify patterns of pathology, including a broad range of gross and microscopic features. SARS-CoV-2 viral nucleic acid sequence in heart tissue was analyzed by PCR testing of formalin fixed paraffin embedded (FFPE) tissue. Electron microscopy (EM) was performed to evaluate for viral localization in myocardium. Immunohistochemistry (IHC) was used to assess for intravascular complement deposits C4d and C3d and to characterize inflammatory cell infiltrates.

**Results:** The mean age of our cohort (n=18) was 66.2 yrs +/- 10.0 (range: 50-89); 14 were male and 4 female; 12 decedents were Hispanic. Fifteen decedents had comorbidities, including diabetes mellitus, hypertension, hyperlipidemia and chronic kidney disease. The mean time from diagnosis to death was 27 +/- 21 days (range: 8-89). The presence of myocarditis was found in 5 cases (27%), consisting of small, focal infiltrates of T cells and histiocytes (by IHC) with minimal myofiber degeneration. Interstitial edema was noted in 10 of 18 cases (56%) and increased vascular macrophages (CD68) were found in 9 of 18 (50%). Vasculitis, intravascular thrombi, and complement deposition (C4d, C3d) were not found. By EM, 1 of 15 cases contained rare viral-type structures (150 nm, with electron dense spikes on the surface, compatible with coronavirus) within stromal cells. PCR testing of FFPE myocardium was positive in 1 of 14 cases.

**Conclusions:** Subsets of hearts of fatal COVID-19 cases exhibit low grade myocarditis, myocardial edema and increased stromal macrophages. Vasculitis, intravascular thrombi and complement activation are not seen. SARS-CoV-2 virus is not commonly detected by PCR or EM in post-mortem myocardium, suggesting a lack of direct viral cytopathic effect in pathogenesis of tissue injury.

## **11 Postmortem Investigation of the Role of MiT/TFE Family of Transcription Factors and Autophagy in COVID-19**

Sonja Chen<sup>1</sup>, Mehran Najibi Kohnehshahri<sup>2</sup>, Weibiao Cao<sup>1</sup>, Mark Birkenbach<sup>2</sup>, Katelyn Dannheim<sup>3</sup>

<sup>1</sup>Rhode Island Hospital, Providence, RI, <sup>2</sup>Brown University, Rhode Island Hospital, Lifespan, Providence, RI, <sup>3</sup>Rhode Island and Hasbro Children's Hospitals, Providence, RI

**Disclosures:** Sonja Chen: None; Mehran Najibi Kohnehshahri: None; Weibiao Cao: None; Mark Birkenbach: None; Katelyn Dannheim: None

**Background:** Autophagy, the degradation of unwanted cell components, is believed to be a key factor in reproduction of coronavirus virion material. Intracellular regulation of autophagy is carried out by members of the microphthalmia/transcription factor E (MiT/TFE) family of transcription factors, including Transcription Factor EB (TFEB) and Transcription Factor E3 (TFE3), which regulate pulmonary cathepsin K, a marker of macrophage differentiation. We investigated these components in autopsied decedents with coronavirus disease 2019 (COVID-19).

**Design:** Immunostains for TFEB, TFE3, and cathepsin K were performed on autopsy lung tissue from six COVID-19 positive (COVID+) decedents (April-July 2020), cases with bacterial, viral, and fungal pneumonia (Oct. 2019-Jan. 2020), and controls with no underlying lung disease (Aug. 2019-Feb. 2020). Staining in macrophages, interstitial cells, and pneumocytes were scored for intensity (0=none, 1=weak, 2=intermediate, 3=strong) and extent (0=0%, 1=<10%, 2=<50%, 3>=50%) and compared between COVID+ patients and the comparison groups.

**Results:** Six COVID+ patients (average age: 59y; range: 38-71y; 3M, 3F) were compared with four normal controls (average age: 59y; range: 14-98y; 4F) and four non-COVID pneumonia cases (average age: 70y; range: 55-87y; combined average age: 65y; range: 14-98y; 1M, 3F). All COVID+ patients showed increased cytoplasmic macrophage and pneumocyte staining for cathepsin K compared to non-COVID pneumonia and controls (p=0.015 and 0.005). Interstitial cells in COVID+ patients also demonstrated cathepsin K expression to a greater intensity and extent (p=0.025 and 0.008). Nuclear cathepsin K staining was decreased in pneumocytes of COVID+ patients (p=0.025) when compared to others. Finally, while not statistically significant, two COVID+ patients demonstrated an endothelial pattern of staining for TFEB; a pattern not seen in the comparison cases.

**Conclusions:** Cathepsin K appears to be upregulated in macrophages and interstitial cells of lungs with COVID-19 pneumonia, compared to other pneumonias and normal controls. TFEB demonstrates occasional endothelial staining in COVID-19 pneumonia, although the significance of this is unclear. Decreased pneumocyte nuclear cathepsin K may be related to cellular injury. These findings suggest upregulation of the autophagy pathway and/or increased macrophage differentiation and help to further elucidate the pathogenesis of COVID-19.

**12 Dermal Microangiopathy of COVID-19: Findings from an International Series of Autopsy and Nailfold Capillaroscopy Studies**

Fernanda Da Silva Lameira<sup>1</sup>, Roberta Gualtierotti<sup>2</sup>, Maryam Sadough<sup>1</sup>, Zaid Khreefa<sup>1</sup>, Bing Han<sup>3</sup>, Nicolo Rampi<sup>4</sup>, Massimo Cugno<sup>2</sup>, Flora Peyvandi<sup>4</sup>, Richard Vander Heide<sup>5</sup>, Sharon Fox<sup>6</sup>  
<sup>1</sup>LSUHSC School of Medicine New Orleans, New Orleans, LA, <sup>2</sup>Università Statale di Milano, Milano, Italy, <sup>3</sup>Louisiana State University, New Orleans, LA <sup>4</sup>Fondazione IRCCS Ca' Granda Ospedale Maggiore Policlinico, University of Milan, Milano, Italy, <sup>5</sup>Louisiana State University Health Sciences Center, New Orleans, LA, <sup>6</sup>SLVHCS/ Louisiana State University, New Orleans, LA

**Disclosures:** Fernanda Da Silva Lameira: None; Roberta Gualtierotti: None; Maryam Sadough: None; Zaid Khreefa: None; Bing Han: None; Nicolo Rampi: None; Massimo Cugno: None; Flora Peyvandi: None; Richard Vander Heide: None; Sharon Fox: *Consultant*, Boehringer Ingelheim

**Background:** Skin involvement in COVID-19 has been described, particularly as chilblain-like erythema, erythema multiforme and urticaria-like lesions. Evidence suggests that endothelial damage may occur in the skin even without the presence of an obvious rash, and as such our aim was to assess the presence of dermal microangiopathy along the spectrum of mild to severe cases of COVID-19.

**Design:** Nailfold skin samples from a series of seven patients with death due to COVID-19 were obtained at autopsy, as well as from one control patient with death due to sudden pulmonary embolism who was negative for SARS-CoV-2 infection. This patient population included males and females, with an age range of 47-76 years. Five of the decedents had identified as black/non-hispanic, one as white/hispanic, one as “other”/hispanic, and one as white. Gross features of the digits at autopsy included occasional darkening of the skin near the nailfold. Skin samples were examined on H&E and with iron stain, in consultation with an experienced dermatopathologist. These findings were compared to a series of nailfold images acquired from fifteen patients with mild COVID-19 in Milan, Italy, with a capillaroscopic system (Inspectis, Sweden).

**Results:** Histologic examination revealed evidence of microvascular damage in the dermal vessels of all COVID-19 cases. This included a mild, mixed superficial dermal perivascular inflammatory infiltrate, at times lining the capillary endothelium, as well as apparent microvascular ectasia. Red blood cell extravasation was rare, though occasional hemosiderin could be seen, as well as dermal edema. A few cases demonstrated microthrombi within vessels. These findings were not seen in the control nailfold sample. On nailfold videocapillaroscopy of mild COVID-19 cases, microhemorrhages were identified with a frequency higher than that seen in the general population. Rarely, enlarged capillary loops were observed. These findings were not typically seen in all digits, but rather in one or a few fingers, and one patient with mild symptoms showed no vascular changes on capillaroscopy.

Figure 1 - 12

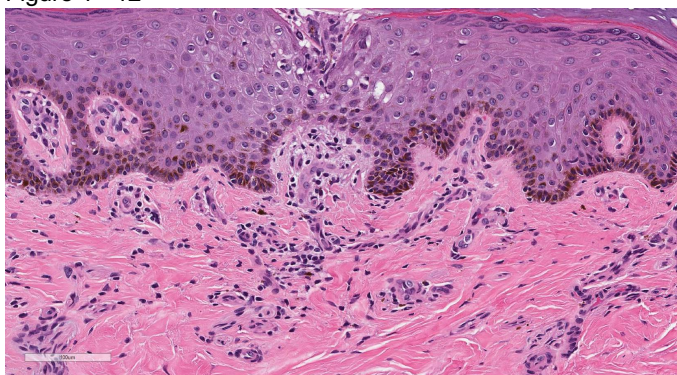
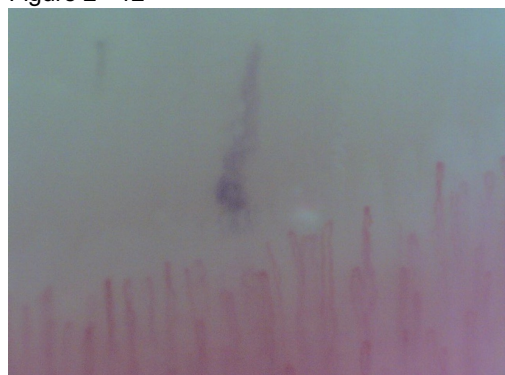


Figure 2 - 12



**Conclusions:** Microvascular damage is a feature of COVID-19, and may be studied through both conventional histopathology and nailfold videocapillaroscopy. The pathologic findings from our collaborative study provide evidence for the involvement of small vessels within the nailfold dermis in both mild and severe cases, and provide a histologic correlate of capillaroscopic findings that may be non-invasively acquired in clinic patients.

**13 Pulmonary Pathology in Long-Haul COVID-19 at Autopsy**

Fernanda Da Silva Lameira<sup>1</sup>, Maryam Sadough Shahrizadi<sup>2</sup>, Richard Vander Heide<sup>2</sup>, Sharon Fox<sup>3</sup>  
<sup>1</sup>LSUHSC School of Medicine New Orleans, New Orleans, LA, <sup>2</sup>Louisiana State University Health Sciences Center, New Orleans, LA, <sup>3</sup>SLVHCS/ Louisiana State University, New Orleans, LA

**Disclosures:** Fernanda Da Silva Lameira: None; Maryam Sadough Shahrizadi: None; Richard Vander Heide: None; Sharon Fox: *Consultant*, Boehringer Ingelheim

**Background:** The pulmonary pathology of severe acute SARS-CoV-2 infection has been described over the past year in numerous autopsy series around the world, with diffuse alveolar damage, pulmonary vascular thrombosis, and microangiopathic changes among the most common findings. An important question is how the lungs may be affected by COVID-19 in the so called “long-haul” cases, in which patients appear to recover from the initial severe infection, but still experience the sequelae of the disease many weeks to months later. Herein we present the first series of autopsy cases demonstrating the potentially severe pulmonary pathology of long-haul COVID-19 infection.

**Design:** Autopsies were performed on a series of male and female decedents, between 31 and 61 years of age, having previously been diagnosed with SARS-CoV-2 infection by nasopharyngeal swab RT-PCR. The known comorbidities of the decedents included systemic hypertension, and type 2 diabetes, but none had pre-existing pulmonary disease, or a significant history of smoking. All decedents had a prolonged period of hypoxic respiratory illness prior to death (between 29 to 112 days following diagnosis of SARS-CoV-2 infection), some having been tested a second time, with a negative nasopharyngeal swab for SARS-CoV-2 despite continued impaired respiratory function. Consent for autopsy was non-restricted by the next of kin, and this study was determined to be exempt by the IRB.

**Results:** The pulmonary findings in all cases demonstrated areas consistent with diffuse alveolar damage in the late proliferative or organizing stages, with other regions appearing as dense fibrous bands, most consistent with a severe organizing pneumonia. In at least one case, the dense fibrotic pattern appeared to obliterate the alveolar spaces, with neighboring regions of ongoing fibroplasia, resulting in a cause of death due to extensive fibrosing organizing pneumonia. In another case, the lung injury pattern was accompanied by a significant increase in neutrophils, evidencing a concomitant pneumonia entrapped within these regions of organization.

Figure 1 - 13

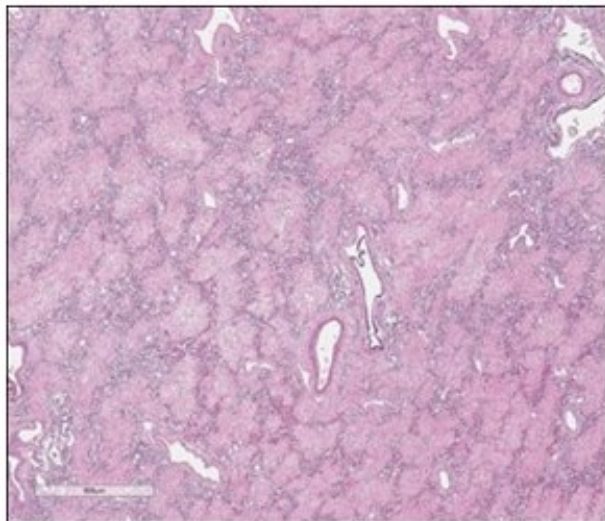


Figure 2 - 13



**Conclusions:** This study is the first to examine the pulmonary pathology associated with hypoxic respiratory failure in so-called “long-haul” COVID-19 patients, who had initially demonstrated a recovery from SARS-CoV2 infection, and later succumbed to the sequelae of the disease. We provide pathologic evidence that SARS-CoV2 can cause severe, and potentially long-lasting fibrotic damage to the lungs.

#### **14 No Specific Pathology or Detectable SARS-CoV-2 Spike Protein in Gastrointestinal Tracts from Ten COVID-19 Autopsies**

Armando del Portillo, Columbia University Irving Medical Center, New York, NY

**Disclosures:** Armando del Portillo: None

**Background:** Coronavirus disease 2019 (COVID-19) is caused by the SARS-CoV-2 virus and has led to a pandemic that has infected over 43 million people worldwide, resulting in 1.1 million deaths thus far. The virus enters cells through the angiotensin-converting enzyme 2 (ACE2), which is expressed in type II alveolar cells of the lungs, but also in epithelial cells of the stomach and small and large bowel. Swallowing SARS-CoV-2-laden mucus secretions may introduce infectious virus to the gastrointestinal (GI) tract and thus has the potential to cause disease in these organs.

**Design:** This study aimed to determine what, if any, pathologic findings occur in the GI tracts of patients who died with COVID-19. Ten consecutive COVID-19 positive autopsies that had a post-mortem interval <10 hours were selected for study. Full thickness sections were taken from the esophagus, stomach, small intestine, and colon. H&E-stained slides were scanned, and the digital images were reviewed for pathology. Samples with severe autolysis were excluded from further study. Thirty-two sections from the GI tracts from 10 patients, along with positive lung controls, were stained for SARS-CoV-2 spike protein, using the mouse monoclonal antibody 1A9 (GeneTex, 1:1000, 30 min, Leica Bond platform). The 32 sections comprised of samples from esophagus (9), stomach (7), small bowel including duodenum or ileum (5), and colon (11).

**Results:** One stomach section showed chronic inactive gastritis. Patchy, mild, non-specific, chronic inflammation was seen in samples from the esophagus, stomach, and small bowel. No significant pathologic change was seen in the colon samples. No specific epithelial staining for SARS-CoV-2 spike protein was seen in any of the 32 sections. Although a faint, weak stain was seen in many areas of smooth muscle, no specific staining was seen in any other cell type.

**Conclusions:** No specific pathology or SARS-CoV-2 spike protein was detected in the GI tracts from 10 autopsy patients who had COVID-19. Although the epithelia from the GI tract express the viral receptor ACE2, this study shows no evidence of infection of the GI tract by this virus. Limitations include sensitivity to detect SARS-CoV-2 spike protein and post-mortem degradation effects.

#### **15 Abdominal Apoplexy: An Autopsy Case Series with Molecular Analysis**

Samreen Fathima<sup>1</sup>, Sarah Glogowski<sup>1</sup>, Muhaymin Syed Abdul-Moheeth<sup>2</sup>, Pedro Pacheco N<sup>2</sup>, Medhat Askar<sup>3</sup>, Joseph Guileyardo<sup>1</sup>

<sup>1</sup>Baylor University Medical Center, Dallas, TX, <sup>2</sup>Texas A&M University, Dallas, TX, <sup>3</sup>Baylor University Medical Center Dallas, Dallas, TX

**Disclosures:** Samreen Fathima: None; Sarah Glogowski: None; Muhaymin Syed Abdul-Moheeth: None; Pedro Pacheco N: None; Medhat Askar: None; Joseph Guileyardo: None

**Background:** Abdominal apoplexy (AA) refers to nontraumatic hemorrhage from a ruptured intra-abdominal artery or vein. The definition excludes ruptured aortic aneurysms or dissections, bleeding from gynecologic lesions such as ectopic pregnancy, and bleeding from visceral malignancies. Despite the small size of the ruptured vessel, this condition carries a high risk of fatal exsanguination.

The pathogenesis of AA remains poorly understood, and proposed causes include systemic or portal hypertension, atherosclerosis, various forms of vasculitis, fibromuscular dysplasia and hereditary disorders such as Marfan and Ehlers-Danlos syndromes.

**Design:** In order to explore potential genetic etiologies of AA, we performed whole exome sequencing (WES) by next-generation sequencing of five previously diagnosed autopsy cases of abdominal apoplexy.

The autopsy files of were searched from January 1, 2010 through December 31, 2019, for cases of AA. WES of the AA cases using genomic DNA extracted from formalin fixed-paraffin embedded skeletal muscle in all cases and peripheral whole blood for comparison in one of the cases was performed. Targeted WES with ACMG (American College of Medical Genetics) sample classifier with VarSEQ algorithm was used to analyze the variants.

**Results:** One thousand autopsies were performed during the study period with 5 (0.5%) identified cases of abdominal apoplexy. All were women, ranging from 42 to 84 years or age. The source of hemorrhage was the gastro-duodenal artery (three cases), the splenic artery (one case) and a mesenteric-portal vein (one case). A novel mutation involving the COL3A1 gene, consistent with the Ehlers-Danlos syndrome, was found in the case of splenic artery rupture.

WES identified several additional potentially significant variants. An LIMS1 variant was shared among 3 cases and the ARHGEF5 variant was present in 2 cases. NOTCH2 and EPPK1 variants were seen in all 5 cases. The potential significance of these variants warrants further study. Final classification of potentially significant variants depends on continued accumulation of phenotypic and genetic data.

**Conclusions:** AA is probably multifactorial in origin; however, accurate diagnosis is essential for accurate death certification and appropriate genetic counseling for potentially affected family members.

## **16 Super-Spreading Events of an Earlier Era: A Re-examination of Autopsy Cases of Typhoid Fever During the Time of Typhoid Mary**

Leah Geiser Roberts<sup>1</sup>, Jonathan Melamed<sup>2</sup>

<sup>1</sup>NYU Langone Health, New York, NY, <sup>2</sup>New York University, New York, NY

**Disclosures:** Leah Geiser Roberts: None; Jonathan Melamed: None

**Background:** Mary Mallon was termed Typhoid Mary for her role in spreading typhoid fever in the early 1900s. Dr. Soper identified her as a super spreader based on her occupation as a cook in many households that were afflicted. She was subsequently sentenced to enforced confinement to reduce the risk of her continuing to spread disease, yet her exact toll is not fully determined. Pre-antibiotic era, typhoid fever resulted in ~10% mortality. While Mallon has been implicated in 53 cases of typhoid fever, she was implicated in only 3 deaths. We examined the autopsy records of a hospital within 1 mile of her home in NYC to identify whether any deaths from typhoid fever could be associated with her geographically. We anticipated the challenges raised by limited availability of records, however derived inspiration from John Snow's use of geolocation data to elucidate the mechanism of cholera spreading events.

**Design:** We investigated all autopsy records of a public hospital located within 1 mile of the home of Mary Mallon from 1905-1907, prior to her confinement. We recorded name, age, and district of the deceased. We then investigated death and voting registry records for information on the deceased and newspapers for any obituaries. We derived home/work addresses, ethnicity and ages of the deceased to identify any clusters, and to geolocate in relation to Mallon's home/work addresses in the 3 weeks prior to death.

**Results:** We found 22 patients that died of typhoid fever as follows: 20 M, 2 F, ages 23-47, 9 of Irish ethnicity. We grouped them into 4-week clusters of dates of death and identified 7 clusters. The ages in these clusters more closely approximated each other as compared to the overall group. Socioeconomic information was available in a minority of the group, however their treatment and subsequent death in a public hospital suggested their employment in low earning jobs, similar to Mallon.

**Conclusions:** The relatively low death count attributed to Mallon remains unexplained. The patients that died during the time that Mallon lived in the neighborhood of the hospital raise possibility for an association. Archived public records have provided further information on some of the deceased and delineation of small clusters, however insufficient evidence has been derived yet to make any association. Further efforts are planned to search



other city and hospital records to identify the estimated 2-3 unaccounted deaths that may be associated with Typhoid Mary.

### **17 Consent for Autopsy: The Role of the Pathologist and Pathology Resident**

Amanda Kardys<sup>1</sup>, Donald Dukette<sup>2</sup>, Sharon Mount<sup>3</sup>

<sup>1</sup>Larner College of Medicine at the University of Vermont, Burlington, VT, <sup>2</sup>The University of Vermont Health Network, Burlington, VT, <sup>3</sup>University of Vermont Medical Center, Burlington, VT

**Disclosures:** Amanda Kardys: None; Donald Dukette: None; Sharon Mount: None

**Background:** The autopsy is an essential component of training in pathology and requires consent from the decedent's next of kin. There is debate in the literature concerning the role of pathologists in this process. Furthermore, there is little information addressing resident experience as it involves obtaining autopsy consent. The purpose of this research was to better characterize the pathologist's involvement in obtaining autopsy consent and to assess the experience and anxiety level of pathology residents involved with this task.

**Design:** Autopsy consent forms from 2017-2019 were reviewed for 383 consecutive autopsies performed at an academic teaching hospital. A 10-question online survey was sent to 16 pathology residents requesting information regarding their role in obtaining consent from next of kin as well as their attitudes and comfort level. Included in the survey were the College of American Pathologists (CAP) guidelines for obtaining autopsy consent. The primary speaker was defined as the individual who took responsibility for the majority of the conversation, as distinct from the person listening as witness.

**Results:** Members of the pathology department obtained consent in 53% of autopsies (204/383), the majority of which were conducted over the phone. The survey was completed by 13/16 pathology residents. There were 3 residents who never participated as primary speaker and 5 residents who were the primary speaker for less than 25% of the consents. Only 2 residents were the primary speaker for greater than 50% of the consents. A comfort level of 3 or 4 was reported by 8/10 residents when speaking with the next of kin (Likert scale of 1-5 with 1 = not comfortable at all and 5 = extremely comfortable). 69% (9/13) of residents were unaware of CAP autopsy consent guidelines and 77% (10/13) residents reported they found these guidelines extremely helpful.

**Conclusions:** The work of the pathologist and the pathology resident includes more than performing the autopsy procedure and reporting the findings. At an academic hospital, the autopsy pathologist's responsibilities may involve obtaining consent from the next of kin, a skill that must be taught to trainees on the autopsy rotation. As residents do not feel entirely comfortable in performing this task, increased training, standardized guidance and awareness of the CAP guidelines may increase skill and comfort level for residents involved in this process.

### **18 Post-Mortem Survey of Hemoglobin A1c, Non-Alcoholic Steatohepatitis and Liver Fibrosis Within A General Population**

Kristina-Ana Klaric<sup>1</sup>, Jacqueline Parai<sup>2</sup>, Charis Kepron<sup>3</sup>, Alfredo Walker<sup>4</sup>, Christopher Milroy<sup>2</sup>

<sup>1</sup>University of Ottawa, Ottawa, Canada, <sup>2</sup>The Ottawa Hospital, Ottawa, Canada, <sup>3</sup>The Ottawa Hospital, Eastern Ontario Regional Laboratory Association, Ottawa, Canada, <sup>4</sup>Ottawa Hospital, University of Ottawa, Ottawa, Canada

**Disclosures:** Kristina-Ana Klaric: None; Jacqueline Parai: None; Charis Kepron: None; Alfredo Walker: None; Christopher Milroy: None

**Background:** Non-alcoholic fatty liver disease and steatohepatitis (NASH), and liver fibrosis, are associated with diabetes mellitus and obesity. Using histologic assessment, autopsy studies in the 1970s-1990s found a prevalence of fatty liver disease of 16-24% of the general population. More recent studies, using radiologic imaging and serology, suggest a prevalence of fatty liver ~20-35%, NASH ~5%, and advanced fibrosis ~2-3%, likely reflecting increasing rates of obesity and diabetes. We sought to assess the prevalence of NASH and liver fibrosis and to identify clinical and biochemical factors predictive of NASH and liver fibrosis in a general autopsy population.

**Design:** Prospective study of consecutive medicolegal autopsies over a 1-year period. History of liver disease, alcoholism, age <18 years, and factors precluding postmortem HgA1c analysis or liver histology were criteria for

exclusion. Liver sections (stained with H & E and Masson trichrome) were scored for fibrosis, inflammation, and steatosis using a modified NASH Clinical Research Network scoring system (ballooning could not be reliably assessed in this autopsy material). NASH was defined as a total score of  $\geq 4$  and moderate/severe fibrosis as a fibrosis score of 3-4. Stepwise logistic regression was used to identify associations between NASH or moderate/severe fibrosis and clinicopathological parameters.

**Results:** Of 376 cases that met the inclusion criteria, 86 (22.9%) were classified as NASH. Prevalence of diabetes, mean BMI and mean postmortem HgA1c were significantly higher in NASH cases (39.5%, 32.3 kg/m<sup>2</sup> and 6.88%, respectively) than in non-NASH cases (12.1%, 27.0 kg/m<sup>2</sup>, and 5.73%, respectively) (all  $p < 0.0001$ ). Similarly, decedents with moderate/severe fibrosis (n=26, 6.9%) had higher prevalence of diabetes, mean BMI and mean HgA1c (50%, 31.4 kg/m<sup>2</sup>, and 6.7%, respectively) compared to those with no/mild fibrosis (16%, 28 kg/m<sup>2</sup>, and 5.9%, respectively) ( $p < 0.0001$ ,  $p = 0.02$  and  $p = 0.014$ , respectively). Following logistic regression, HgA1c  $\geq 7\%$  was found to be an independent predictor of NASH (OR 5.11, 95% CI 2.61-9.98) and advanced fibrosis (OR 3.94, 95% CI 1.63-9.53).

**Conclusions:** The prevalence of NASH and advanced fibrosis was higher in our general adult autopsy population compared to published estimates. This is one of the first large series with histologic evaluation to show that HgA1c  $\geq 7.0\%$  (poorly controlled diabetes mellitus) is independently associated with NASH and advanced fibrosis.

## 19 Postmortem Clot or Antemortem Thrombus: An Updated Description of a Primordial Dilemma

Alison Krywaczyk<sup>1</sup>, Carmela Tan<sup>1</sup>, E. Rene Rodriguez<sup>2</sup>

<sup>1</sup>Cleveland Clinic, Cleveland, OH, <sup>2</sup>Cleveland Clinic Foundation, Cleveland, OH

**Disclosures:** Alison Krywaczyk: None; Carmela Tan: None; E. Rene Rodriguez: None

**Background:** Distinguishing postmortem clot (PMC) from true antemortem thrombus (AMT) is of critical importance when determining cause of death. Classic PMC is described as “chicken fat” or “red cruor”. The presence of “lines of Zahn” is considered pathognomonic for AMT. However, Zahn’s original report has no illustrations, and the literature shows heterogeneous interpretations of the term. Thrombi with organization are easily characterized as antemortem, but acute thrombi can be difficult to discern from PMC. Clarifying the definition of lines of Zahn and identifying microscopic features that reliably distinguish PMC from AMT will aid pathologists in interpreting the significance of clots found at autopsy.

**Design:** PMC collected from the right heart in 50 hospital autopsies was sampled (one cassette per 5g of clot). Surgical pathology of 25 arterial thrombi and 25 venous thrombi from autopsy and surgical specimens were reviewed. CD61 immunostain and PTAH stain were used to assess platelet and fibrin distribution, respectively. Histologic features and fibrin/CD61 staining pattern of PMC and AMT were compared.

**Results:** Light microscopy showed: 1. Chicken fat PMC is a delicate meshwork of fibrin and platelets, with scattered erythrocytes, leukocytes, and peripherally-located karyorrhectic neutrophils entrapped in dense fibrin; 2. Bone marrow elements without adipose tissue were commonly identified in chicken fat PMC; 3. Red cruor PMC was formed of aggregates of erythrocytes with rare admixed leukocytes and thin strands of fibrin and platelets, potentially mimicking lines of Zahn; 4. Arterial and venous AMT showed thick, serpiginous aggregates of platelets wrapped by fibrin, with adjacent erythrocytes and leukocytes (neutrophil karyorrhexis was seen in nearly all cases, distributed throughout the thrombi); 5. CD61 stained AMT in a tigroid/stratified pattern, while both chicken fat and red cruor PMC had a speckled staining pattern.

**Conclusions:** Chicken fat PMC is unlikely to be mistaken for AMT. However, red cruor PMC may be ambiguous and can have deposition of fibrin-platelet layers mimicking lines of Zahn. True lines of Zahn in AMT are thick aggregates of platelets wrapped by fibrin; neutrophil karyorrhexis present throughout the thrombus is a distinctive feature of AMT. While karyorrhexis could be seen in chicken fat PMC, it was only at the periphery of the clot. Pathologists must be aware of the morphologic overlap between AMT and PMC. Thorough histologic sampling with fibrin and CD61 staining are helpful to make the distinction.

## 20 Revisiting the Autopsy Report: Images of Tuberculosis in a Bygone Era

Jonathan Lai<sup>1</sup>, Sarah Sutherland<sup>2</sup>, Richard Fraser<sup>3</sup>

<sup>1</sup>McGill University Health Centre, McGill University, Montréal, Canada, <sup>2</sup>McGill University, Montreal, Canada, <sup>3</sup>McGill University Health Centre, Montreal, Canada

**Disclosures:** Jonathan Lai: None; Sarah Sutherland: None; Richard Fraser: None

**Background:** The Pathology Department of the Royal Victoria Hospital (RVH) was established at the Hospital's inception in 1893. Autopsies and the bound books that documented their results began at approximately the same time. The first reports consisted of a pathological diagnosis list, case synopsis, clinical history and gross/microscopic descriptions. In the early 1940s, selected reports were also illustrated by high quality black and white photographs, including examples of both common and rare diseases. One of the most frequent of these was tuberculosis (TB). We investigated the RVH autopsy records to identify the types of disease illustrated, concentrating on the frequency and patterns of tuberculous disease.

**Design:** We reviewed autopsy records in the RVH archives from 1946-1956. All cases that included photographs were identified. Photographs were scanned, and the pertinent diagnoses and demographic information were recorded. Cases that had a diagnosis of TB were selected for detailed analysis.

**Results:** 4713 autopsies were identified, of which 997 (21%) had photographs; 68 (7%) of these were cases of TB. Within the TB cases, patient age ranged from 5.5 months to 76 years; photographed organs included lung (52 cases), brain (13), spleen (13), kidney (6) and liver (4). Pulmonary images showed a variety of disease patterns, including fibrocaceous, miliary, cavitory (+/- hemorrhage), tuberculoma, pleuritis/pleural fibrosis, tracheobronchial ulceration, healed (calcified granuloma, bronchiectasis) and nodal. Other organs also showed typical pathological patterns, such as basal meningitis and hydrocephalus, pyelonephritis, and miliary nodules.

Figure 1 - 20



Figure 1: Primary tuberculosis showing a Ghon focus in the right lung periphery. Necrotic and caseated lymph node disease and miliary nodules.

Figure 2 - 20



Figure 2: Fibrocaceous tuberculosis of the left lung with fatal intra-cavitary haemorrhage. Small foci of tuberculous spread in the right lung and necrotic subcarinal lymph nodes are also evident.

**Conclusions:** In early 1900, Montreal had one of the highest prevalence rates of TB in North America. Although this decreased over the following decades, the disease was still a significant cause of illness in the city in the 1940s. In fact, during the period in this study, it was an important contributory cause of death in 1.5% of patients autopsied at the RVH. The photographs in the autopsy record books were probably included as a teaching aid for pathology residents and medical students. Since TB prevalence and mortality have declined considerably since the

1950s, medical trainees now have little exposure to gross specimens that illustrate TB. In addition to providing insight into the spectrum and prevalence of such disease in mid-20<sup>th</sup> century Montreal, the photographs are thus still a useful aid in pathology education.

## **21 Rectal Swab SARS-CoV-2 Testing and Histologic Findings in the Small Intestine of 18 Autopsy Patients**

Lawrence Lin<sup>1</sup>, Sunjida Ahmed<sup>1</sup>, Kristen Thomas<sup>1</sup>, Melissa Guzzetta<sup>2</sup>, Deepthi Hoskoppal<sup>3</sup>, Margaret Cho<sup>1</sup>, Yvelisse Suarez<sup>4</sup>, Weiguo Liu, Cristina Hajdu<sup>5</sup>, Neil Theise<sup>6</sup>, George Jour<sup>7</sup>, Suparna Sarkar<sup>1</sup>, Wenqing (Wendy) Cao<sup>1</sup>

<sup>1</sup>NYU Langone Health, New York, NY, <sup>2</sup>NYU Langone Health, Westfield, NY <sup>3</sup>New York University Langone Medical Center, New York, NY <sup>4</sup>NYU Medical Center, New York, NY, <sup>5</sup>New York University School of Medicine, New York, NY, <sup>6</sup>Beth Israel Medical Center, New York, NY <sup>7</sup>New York University, New York, NY

**Disclosures:** Lawrence Lin: None; Sunjida Ahmed: None; Kristen Thomas: None; Melissa Guzzetta: None; Deepthi Hoskoppal: None; Margaret Cho: None; Yvelisse Suarez: None; Weiguo Liu: None; George Jour: None; Suparna Sarkar: None; Wenqing (Wendy) Cao: None

**Background:** Digestive symptoms are often seen in COVID-19 patients with poor outcomes. The Viral RNA is mostly positive in the stool of these patients, and has a longer delay before viral clearance. However, its diagnostic value and significance for guiding clinical treatment remain unknown. And the pathologic alterations in the GI tract in COVID-19 patients have not been well defined. We evaluated rectal swab SAS-CoV-2 test and histopathologic changes in the small intestine in autopsy patients.

**Design:** 18 autopsy cases with confirmed SAS-CoV2 infection were included. Nasal, bronchial, and rectal swab SARS-CoV-2 PCR were performed at the time of autopsy. Clinical information included demographics, comorbidities, presenting symptoms, related laboratory tests were collected. Histopathologic evaluation was performed and correlated with clinical properties.

**Results:** 83% (15/18) of patients were male. Median age is 50 years. 7/18 (38.9%) patients had diarrhea in addition to cough, fever and other symptoms. Except in one case, all patients had underlying comorbidities of diabetes, hypertension and /or obesity. In the small intestine, acute inflammation was not seen in any cases. 5/18 displayed mild and one showed moderate chronic inflammation. Hypermucinous change was found in six patients but not associated with diarrhea. 3 cases had microthrombi identified in the sections. Notably, obviously increased D dimer in lab tests were noticed in all patients. Postmortem 17/17 (100%) nasal, 18/18 (100%) bronchial and 7/16 (43.8%) rectal swabs showed SARS-CoV-2 PCR positivity. 3 of 7 (42.9%) patients with diarrhea are positive in rectal swab for SARS-CoV-2.

**Conclusions:** There are no specific COVID-19 changes in the small intestine. More investigations are needed, especially on tissues from different locations of the GI tract. Data from rectal swab testing suggests that it is not ideal for diagnosing COVID-19, guiding treatment, or predicting small intestinal pathology.

## **22 Drowning in Vermont: A Descriptive Epidemiologic and Autopsy Study Reveals Racial Disparity in a Predominantly White State**

Rachel Martindale<sup>1</sup>, Lauri McGivern<sup>2</sup>, Sharon Mount<sup>1</sup>

<sup>1</sup>The University of Vermont Medical Center, Burlington, VT, <sup>2</sup>Office of Chief Medical Examiner, Burlington, VT,

**Disclosures:** Rachel Martindale: None; Sharon Mount: None

**Background:** Accidental drowning is a significant public health problem, and is one of the top three causes of unintentional injury resulting in death in persons under the age of 30 in the USA. Studies have demonstrated a racial disparity among drowning victims. Circumstances surrounding drowning in a predominantly White and rural state may differ from other communities. A better understanding of the epidemiology of drowning is needed to inform public health initiatives aiming to reduce accidental drowning.

**Design:** Drowning deaths in Vermont from 2009 through 2017 were identified by computer search performed at the Vermont State Health Department. Death certificates, medical examiner investigations, and autopsy reports from these drowning deaths were reviewed. Suicide deaths were excluded from the study. Gender, age, race, state of residence, and location of the drowning were recorded and classified using Excel software. Demographics of our state were obtained from review of 2020 projected census data.

**Results:** From 2009 through 2017, there were 119 deaths due to drowning in Vermont. The manner of death was reported as Accident: 87, Suicide: 19, Undetermined: 12 and Natural: 1. Our study group consists of the 100 drowning cases that were not suicides. The most common location for drowning was natural bodies of water, such as rivers, ponds and lakes. There were 4 drownings in pools, 3 in bathtubs, 4 in reservoirs, 1 in a flooded roadway, and 1 in a flooded yard. Our study group contains 82 males and 18 females. 15 decedents were children (age 0-18 years), and 85 were adults (>18 years). There were 12 non-White persons, including 2 Asian, 1 Chinese, and 9 Black individuals. 16 persons were listed as out of state residents. Review of 2020 projected Census data showed the population of our state to be: White 94.2%, African American 1.4%, American Indian/Alaska 0.4%, Asian alone 1.9%, Two or more races 2%, White alone, not Hispanic or Latino – 92.6%.

**Conclusions:** The epidemiology of drowning in Vermont is similar to other US reports, in regards to male predominance and racial disparity. Although African Americans account for 1.4% of our population, this racial group made up 9% of our accidental drowning deaths. Unlike much of the country, drowning deaths in pools are rare in our rural state, and children do not form the highest risk group. Out of state residents composed a significant proportion of the drowning victims (16%).

Even in a state that is 94.2% White, public health initiatives aimed at reducing drowning deaths are needed to address racial and ethnic disparities. In addition, given the rural nature of Vermont, preventive measures should perhaps focus less on pool safety and more on high risk behaviors of males in natural water settings, with particular attention to risk to out of state visitors.

### **23 COVID-19 Autopsy Findings: A Case Series from Houston, TX**

Michelle McDonald<sup>1</sup>, Songlin Zhang<sup>2</sup>, L. Maximilian Buja<sup>2</sup>, Bihong Zhao<sup>1</sup>

<sup>1</sup>The University of Texas Health Science Center at Houston McGovern Medical School, Houston, TX, <sup>2</sup>The University of Texas Health Science Center at Houston, Houston, TX

**Disclosures:** Michelle McDonald: None; Songlin Zhang: None; L. Maximilian Buja: None; Bihong Zhao: None

**Background:** As the COVID19 pandemic spread around the globe causing major morbidity and mortality, the value of the autopsy has once again been highlighted. Autopsy of deceased victims with the disease is of paramount importance for gaining knowledge of its pathogenesis and pathophysiology. This abstract collates the patient characteristics and pathological findings from 34 autopsy patients with COVID-19 from a single teaching institution.

**Design:** All autopsies with positive COVID 19 PCR test result were included in this study. The clinical information was collected from medical chart, and pathology findings were summarized.

**Results:** Total 34 cases including 11 full autopsies, 22 without brain and 1 heart only. In all cases COVID-19 was listed among the primary or immediate causes of death. In 11 cases, acute respiratory failure purely due to COVID-19 was the mechanism. Other cases included 13 superimposed infection/sepsis, 4 exacerbation of chronic heart conditions, 6 CVAs, and 2 due to pulmonary embolism.

Pulmonary findings were available for 33 cases. DAD was found in 31 (93%). Isolated early (hyalinizing) stage DAD was seen in 11 (33%), isolated late (fibrotic) stage DAD was seen in 6 (18%), and the remaining 14 (42%) had mixed findings of various degrees along the spectrum from early to late. Bacterial pneumonia was identified in 23 (69%) and fungal infection was found in 3 (9%). Microthrombi were noted in 17 (51%), lymphocytic pneumonitis in 10 (29%), and pleuritis in 5 (15%).

IHC stains for SARS-CoV-2 were performed on 14 cases using 3 different antibodies (AbboMax, CA, S2 and N1; GeneTex, GTX632604), and only 2 cases had positive IHC staining. The two IHC positive cases died 5 and 2 days after testing positive, respectively. All other 12 cases with negative IHC had longer intervals (from 8 to 57 days) except one, which had a 1 day interval.

# ABSTRACTS | AUTOPSY AND FORENSICS

Case	DemoGRAPHICS	BMI	PMH	Symptoms before admission (Days)	Admitted (Days)	Positive test to death (Days)	TreaTment	LYMPH nORM 1.0-5.5 k/cmm	DD nORM <0.5 ug/mL FEU	Troponin I norm <0.4 ng/mL	BNP nORM
1	70 AM	22.5	HTN, DM, Dementia (vasc & Alz)	2	8	8	none	0.9	ND	ND	ND
2	71 BM	27.7	HTN, DM, Dementia (vasc & Alz), CVA, COPD, HLD, colon cancer	0	5	15	Hy	0.6	ND	0.02	ND
3	53	31.5	HTN, DM	5	41	41	V, P, Hy, ECMO	0.8	ND	ND	ND
4	BF 53 BM	36	HTN, DM, MI s/p PCI, pneumonectomy	2	16	12	V, ECMO	0.9	ND	ND	ND
5	59 BM	33.8	HTN, DM, CAD s/p CABG, mitral valve stenosis s/p repair	3	5	5	V, P, R	0.4	5.23	0.19	575
6	39	41.4	Lupus, ESRD, liver cirrhosis, hypothyroid	4	12	6	V, P	0.4	17.6	ND	318
7	BF 51 HM	28.9	HTN, substance abuse	0	2	2	V, D	0.2	ND	0.1	ND
8	55 WF	33.9	HTN, DM	5	57	57	V, P, Hy, D, ECMO	0.6	0.81	0.04	ND
9	36 HF	28.6	DM, Postpartum (2 mo)	14	1	1	V	5.9	20	2.43	ND
10	79 HM	27.8	HTN, CVA, HLD, Hypothyroid, BPH	0	4	4	None	0.8	1.79	0.09	75
11	71 HM	33.7	HTN, DM, CAD s/p CABG, CVA, PVD, HLD, CKD -3	0	29	2	V	0.6	ND	1.16	3038
12	73 BM	21.3	HTN, DM, HFrEF, HLD, PAD	3	7	13	V, P, R	0.7	2.78	0.02	321
13	63 WM	51.9	HTN, DM, HLD, CKD	3	21	21	V, P, R, D	0.7	1.61	0.02	ND
14	45 BM	31.6	HFrEF NICM s/p LVAD, ESRD, HLD, DVT, COPD	0	29	29	V, P, D	0.6	ND	ND	979
15	56	86.5	HTN, CVA, asthma, OSA, Schizophrenia, pancreatitis	0	30	30	V, D	0.4	2.35	0.7	128
16	BF 47	71.7	HTN, DM, HLD	7	31	31	V, P, R	1.6	2.52	0.02	8
17	BF 47 HF	33.9		4	21	21	V, P, D	0.8	ND	1.31	186
18	64 HF	29.3	HTN, DM, CVA	0	26	26	V, P, D	1.2	2.24	0.21	1106
19	48 BM	23.8	HTN, NICM s/p LVAD, SAH	1	24	29	V	0.5	1.8	0.02	ND
20	68 HM	29.6	HTN, Chronic back pain	0	33	33	V, P, R, D	0.8	1.14	0.02	ND
21	41 HF	32.7		6	26	25	V, P, Hy, R, D, ECMO	0.7	0.27	0.02	ND
22	50 BM	36.5	HTN, DM	5	45	45	V, P, R, D, ECMO	0.4	0.52	ND	ND
23	32 WF	48	HTN, DM	5	36	36	V, P, R, D	1.2	1.04	0.02	10
24	54 HM	37.5	GERD, lumbar impingement	4	54	54	V, P, R, D	1	0.46	0.02	ND
25	57	24.3	HTN, meningiomas, HLD, substance abuse	0	7	7	V	2.1	ND	0.02	ND
26	BF 57 HF	29	Tumefactive MS, recurrent UTIs	9	48	48	V, P, R	1.6	1.84	0.02	104
27	34 BM	51.7	HTN, HFrEF 2/2 myocarditis	4	10	10	none	0.5	ND	0.06	428
28	62 HM	33.1	HTN, DM, NASH	5	14	14	V, P	1.14	ND	0.02	ND
29	60 HM	40.1	HTN	5	29	29	V, R, D	1.95	20	0.08	ND
30	55 BM	26	CVA, Hep C, cirrhosis	4	23	25	V, R, D	1.26	0.7	ND	ND
31	63	32.8	HTN, DM, COPD	0	0	0	none	ND	ND	ND	ND
32	BF 74 HM	28.9	HTN, DM, COPD	1	31	31	V, R, D	0.59	ND	0.02	ND
33	69 HF	39.4	HTN, DM, HLD	3	58	58	V, R, D	1.38	1.15	0.03	ND
34	55 HF	39.5	DM	6	62	62	V, R, D	1.4	0.5	ND	ND

Abbreviations, listed alphabetically

A: Asian, Alz: Alzheimer's disease, B: black, BMI: body mass index, BNP: brain natriuretic peptide, BPH: benign prostatic hyperplasia, CABG: coronary artery bypass graft, CKD: chronic kidney disease, COPD: chronic obstructive pulmonary disease, CVA: cerebrovascular accident, D: dexamethasone, DD: D-dimer, DM: diabetes mellitus, DVT: deep vein thrombosis, ECMO: extracorporeal membrane oxygenation, ESRD: end stage renal disease, F: female, GERD: gastroesophageal reflux disease, H: Hispanic, HFREF: heart failure with reduced ejection fraction, HLD: hyperlipidemia, HTN: hypertension, Hy: hydroxychloroquine, LVAD: left ventricular assist device, M: male, MI: myocardial infarction, MS: multiple sclerosis, NASH: nonalcoholic steatohepatitis, ND: not done, NICM: nonischemic cardiomyopathy, OSA: obstructive sleep apnea, P: convalescent plasma, PCI: percutaneous intervention, PMH: past medical history, PVD: peripheral vascular disease, R: remdesivir, SAH: subarachnoid hemorrhage, V: ventilation, W: white

Figure 1 - 23

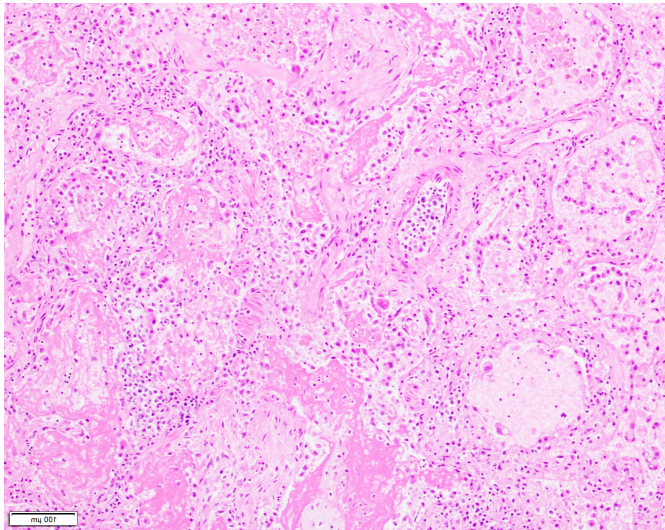
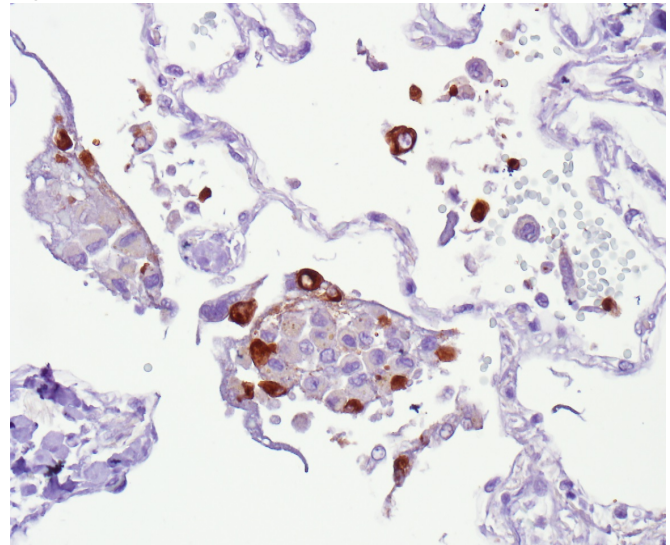


Figure 2 - 23



**Conclusions:** Our autopsies show: 1. SARS-CoV-2 infection causes very severe widespread lung damage; 2. the damage to the lung is disproportional to the viral load. Our IHC results suggests the virus itself is cleared and the ongoing immune response maybe the primary mechanism of continued deterioration; 3. The damage to the lungs is disproportionate to the inflammatory infiltrate. We have to suspect that the cytokine secretion triggered by the infection play a role in the damage. Overall, these results indicate that variable immune response to viral infection significantly influences the clinical course.

## 24 Lack of Focus on Race and Ethnicity in Autopsy Abstracts Accepted by National/International Pathology Conferences Over Five Years

Monica Miyakawa-Liu<sup>1</sup>, Kristinza Giese<sup>2</sup>, Jody Hooper<sup>3</sup>, Marissa White<sup>4</sup>

<sup>1</sup>Ochsner Health System, LA, <sup>2</sup>Washington, DC, <sup>3</sup>Johns Hopkins University, Baltimore, MD, <sup>4</sup>Johns Hopkins University School of Medicine, Baltimore, MD

**Disclosures:** Monica Miyakawa-Liu: None; Kristinza Giese: None; Jody Hooper: None; Marissa White: None

**Background:** Forensic and autopsy pathologists can directly inform and guide public health policy. Consequently, autopsy research focusing on health disparities should be shared and disseminated at meetings of the National Association of Medical Examiners (NAME) and United States and Canadian Academy of Pathology (USCAP). Other medical specialties have performed formal reviews of the coverage of health disparities content. We therefore reviewed the past 5 years of autopsy-focused abstracts presented at the two most prominent pathology meetings in the U.S. to identify possible gaps in this coverage and begin to understand what areas could be better served in review and acceptance of abstracts.

**Design:** Abstracts published at the annual meetings of NAME and the USCAP autopsy category in from 2016-2020 were reviewed to determine if the terms “race,” “ethnicity,” “disparity,” “disparities,” or “equity” were mentioned.

Race, as defined by the Centers for Disease Control and Prevention, includes the following specifiers: American Indian or Alaska Native, Asian, Black or African American, Native Hawaiian or Other Pacific Islander, or White (3). Ethnicity was defined as Hispanic or Latino. Abstracts pertaining to case studies of two or fewer patients were excluded.

**Results:** Only 4.6% (n = 40/870) of published abstracts (excluding case studies) mentioned race or ethnicity over the past five years, of which 5% (n = 34/658) of these were presented at NAME, and 3.5% (n = 6/172) were presented at USCAP (**Figure 1**). Of the 40 total abstracts, 38 mentioned race and 19 mentioned ethnicity (Figure 2). Only 1 abstract directly used "disparity," and no abstracts used "equity." However, 2 additional abstracts were identified to have themes of disparity regarding disproportionate deaths in indigenous communities (**Figure 2**). There were no significant differences between the reporting of race and ethnicity between NAME and USCAP (**Table 1**). There was a significant difference between reporting of ethnicity versus race ( $p < .00001$ ).

	Race Reported			Ethnicity Reported			Race or Ethnicity Reported		
	Y	N	P-value	Y	N	P value	y	n	P value
NAME	32	660	0.5436	16	676	0.7784	34	658	0.5463
USCAP	6	172		3	175		6	172	

Table 1. Fisher exact test of independence was utilized to determine that there were no reporting differences between NAME and USCAP abstracts

Figure 1 - 24

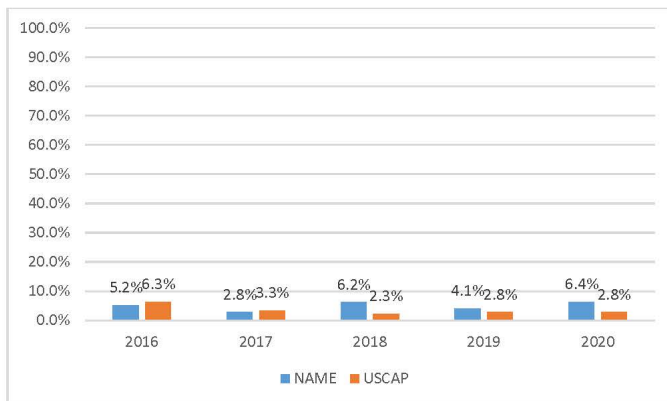
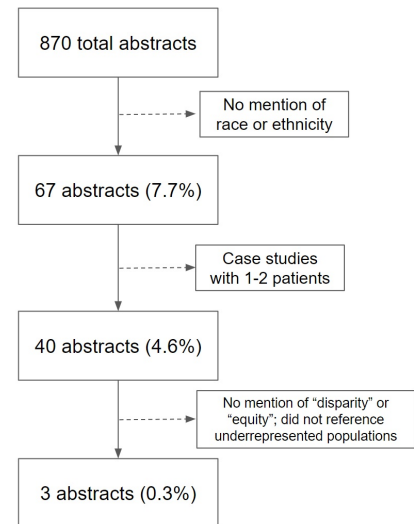


Figure 1. Percentage of abstracts published at annual NAME and USCAP conferences that mention race or ethnicity, excluding case studies

Figure 2 - 24



**Conclusions:** The early, preliminary analysis highlights opportunities for greater attention to racial and ethnic health disparities in autopsy abstracts accepted for presentation at the national meetings of USCAP and NAME. Further studies will be conducted to assess for any broader trends in the presentation of health disparities-focused research and/or educational sessions at national pathology meetings.

**25 Previously Undiagnosed Classic Hodgkin Lymphoma in an Adolescent: A Forensic Autopsy Case Report**

Oluwaseun Ogunbona<sup>1</sup>, Kyle Bradley<sup>2</sup>, Michael Heninge<sup>3</sup>

<sup>1</sup>Emory University School of Medicine, Atlanta, GA, <sup>2</sup>Emory University, Atlanta, GA <sup>3</sup>Fulton County Medical Examiner, Atlanta, GA

**Disclosures:** Oluwaseun Ogunbona: None; Kyle Bradley: None; Michael Heninge: None



**Background:** Few cases of natural sudden death presenting as an undiagnosed lymphoma have been reported in the literature. Herein we provide a report of an asphyxial death caused by classic Hodgkin lymphoma (cHL).

**Design:** Postmortem examination was performed on an 18-year-old female who became unresponsive and was pronounced dead at her residence after having difficulty breathing. In addition to external and internal examinations, microscopic examination was conducted on sections of tissue. Immunohistochemical evaluation using antibodies to CD3, CD15, CD20, CD30, CD45, and PAX5 was performed to confirm the diagnosis.

**Results:** In the weeks prior to death, the decedent reportedly had been eating less, resulting in weight loss, and had increasingly severe respiratory distress that was not medically evaluated. Her family eschewed traditional medical care for personal reasons. External examination revealed an 88-pound, 62.5-inch (body mass index 15.8 kg/m<sup>2</sup>; normal is 18.5-24.9 kg/m<sup>2</sup>) black female with prominent cervical lymphadenopathy and an abdominal rash. Internal examination showed a bulky, dense fibrous and nodular mass filling the mediastinum (up to 15 cm wide) and anterior lower neck. The mass surrounded the internal structures of the anterior neck, encased and compressed the esophagus, compromised the lumen of the trachea in the lower neck, obliterated the pericardial cavity, and encased the great vessels of the heart. Additionally, similar smaller masses (up to 6 cm in greatest dimension) were present in the right and left axillae. Microscopic examination of the masses showed features typical for cHL including large bands of sclerosis, numerous Hodgkin/Reed-Sternberg (H/RS) cells, and a mixed inflammatory cell infiltrate that included many eosinophils. Immunohistochemical stains showed the H/RS cells to be uniformly positive for CD30 and CD15 and negative for CD3, CD20, CD45 and PAX5. Although PAX5 typically shows dim positive staining of H/RS cells in cHL, the overall morphologic and immunophenotypic findings were otherwise typical for cHL.

**Conclusions:** The cause of death in this case is cHL. The terminal mechanism of death is thought to be asphyxiation. The manner of death is natural. This case exemplifies a rare natural death by asphyxiation due to previously undiagnosed cHL in a young patient. In addition, the case provides an example of a malignant neoplasm first diagnosed during forensic postmortem examination.

## **26 Cardiopulmonary Autopsy Findings in COVID-19 Patients from a Single Institution**

Hana Russo<sup>1</sup>, Daniel Stefanko<sup>1</sup>, Andreas Ciscato<sup>1</sup>, Jason Duran<sup>1</sup>, Oluwole Fadare<sup>2</sup>, Omonigho Aisagbonhi<sup>1</sup>, Farnaz Hasteh<sup>1</sup>, Laura Crotty Alexander<sup>1</sup>, Shazia Jamil<sup>1</sup>, Grace Lin<sup>1</sup>

<sup>1</sup>University of California, San Diego, La Jolla, CA, <sup>2</sup>UC San Diego School of Medicine, La Jolla, CA

**Disclosures:** Hana Russo: None; Daniel Stefanko: None; Andreas Ciscato: None; Jason Duran: None; Oluwole Fadare: None; Omonigho Aisagbonhi: None; Farnaz Hasteh: None; Laura Crotty Alexander: None; Shazia Jamil: None; Grace Lin: None

**Background:** Coronavirus disease 19 (COVID-19) is caused by the severe acute respiratory syndrome coronavirus 2 (SARS-CoV-2), which has resulted in a widespread, global pandemic. COVID-19 predominantly manifests in the respiratory tract with the majority of critically ill patients presenting with acute respiratory distress syndrome. Acute cardiac injury, which corresponds to an elevation in high-sensitivity troponin levels, is an important prognostic factor in COVID-19. Therefore, evaluating the cardiopulmonary microscopic changes from autopsies provides a relevant means to understanding the pathogenesis of COVID-19 infection. Although over one million people worldwide have died of COVID-19, autopsy data is still limited.

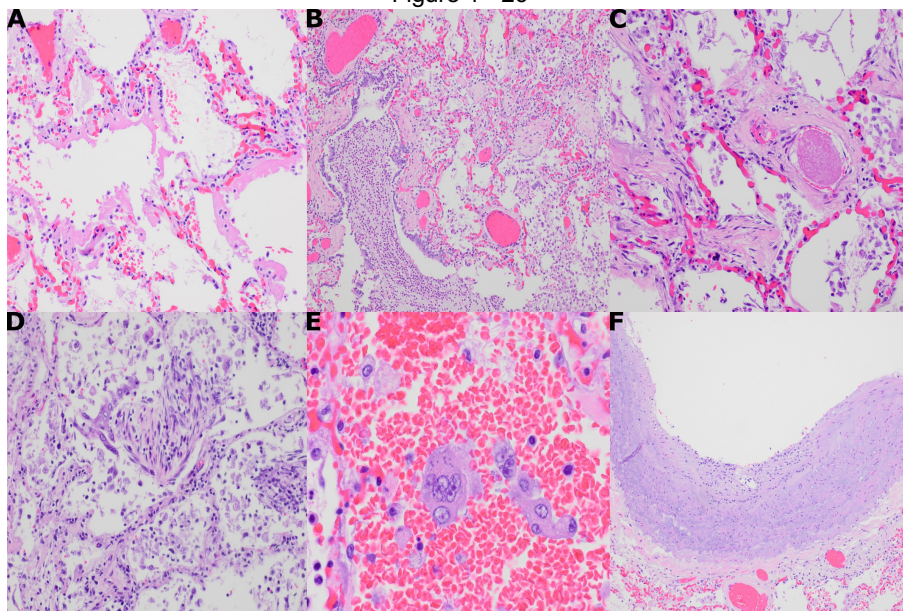
**Design:** For 6 of 67 patients who died of COVID-19 at our institution, permission for an autopsy was obtained from next of kin. There were 1 male and 5 female patients with ages ranging from 44-88 years (mean age: 66.5 years). Gross and microscopic evaluations were performed on the heart and lung tissue from these patients.

**Results:** On gross examination, the lungs were heavy (average weight: 1,676 grams, normal: 685-1050g) with areas of consolidation. Two cases had bilateral pleural effusions. Microscopically, four cases displayed evidence of the exudative phase of diffuse alveolar damage (DAD), including the presence of hyaline membranes (A). One case demonstrated organizing DAD. Superimposed acute pneumonia/bronchopneumonia was identified in four cases (B). All cases displayed fibrin thrombi (C), capillary congestion, and reactive type II pneumocyte hyperplasia (D). Additional histologic pulmonary findings included lymphocytic interstitial inflammation (n=5, D), organizing pneumonia (n=3, B and D), alveolar hemorrhage (n=2), alveolar edema (n=2), multinucleated giant cells (n=2, E),

megakaryocytes (n=4), alveolar septal fibrosis (n=1), and vasculitis (n=1, F). Microscopic evaluation of the heart demonstrated cardiomyocyte hypertrophy in all cases, and five cases had varying degrees of coronary artery disease. Myocarditis and microthrombi were not identified in the heart.

Pulmonary findings	Case 1	Case 2	Case 3	Case 4	Case 5	Case 6	Total	Percent (%)
Hyaline membranes/DAD			X	X	X	X	4	67
Organizing DAD						X	1	17
Reactive pneumocyte hyperplasia	X	X	X	X	X	X	6	100
Acute pneumonia/ bronchopneumonia	X	X		X	X		4	67
Organizing pneumonia	X	X			X		3	50
Microthrombi	X	X	X	X	X	X	6	100
Lymphocytic interstitial inflammation	X	X	X	X		X	5	83
Capillary congestion	X	X	X	X	X	X	6	100
Megakaryocytes			X	X	X	X	4	67
Giant cells		X		X			2	33
Alveolar edema				X	X		2	33
Alveolar hemorrhage				X		X	2	33
Alveolar septal fibrosis		X					1	17
Vasculitis			X				1	17

Figure 1 - 26



**Conclusions:** The most significant histopathologic findings in the COVID-19 autopsies were present in lung tissue. As previously reported in the literature, a common finding was diffuse alveolar damage. However, we also identified microthrombi in all cases and lymphocytic interstitial inflammation in 83 percent of cases. These histopathologic changes may provide mechanistic insight into COVID-19 pathogenesis.

## 27 Correlation of COVID-19 Autopsy and Clinical Findings in Hospitalized Patients in the Academic Center in Metro Atlanta

Conrad Shebelut<sup>1</sup>, Mariko Peterson<sup>2</sup>, Rachel Geller<sup>2</sup>, Mario Mosunjac<sup>2</sup>, Marina Mosunjac<sup>2</sup>  
<sup>1</sup>Emory University Hospital, Decatur, GA, <sup>2</sup>Emory University, Atlanta, GA

**Disclosures:** Conrad Shebelut: None; Mariko Peterson: None; Rachel Geller: None; Mario Mosunjac: None; Marina Mosunjac: None

**Background:** Post-mortem examination of COVID-19 victims has thus far played a valuable role in understanding this disease's pathophysiology. Moreover, correlation with clinical presentation, comorbidities, laboratory data, and the clinical course could further elucidate the causes of sudden and unexplained patient demise.

**Design:** Retrospective analysis of gross and microscopic pathological and corresponding clinical data was performed on autopsy cases of COVID-19 positive decedents. 26 limited autopsies were conducted from April through August of 2020 at three Emory hospital system sites. The electronic medical records were reviewed for demographic data, length of hospital stay, COVID-19 infection prior to death, reported clinical presentation, reported comorbidities, body mass index, intubation, and treatment. Daily laboratory values for D-dimer, platelets, neutrophils, and lymphocytes were collected.

**Results:** autopsy series of 26 COVID-19 positive patients had an equal proportion of male to female patients, predominantly black (80.8%), who had an average age of 64.61 years. Hypertension was the most common comorbidity, followed by obesity, chronic kidney disease, and diabetes. 84.6% of patients had at least three comorbidities. Prevalent presenting symptoms were dyspnea, cough, and fever. On average, patients had hospital stays of 15 days, and all required ventilator support (Table 1). Nearly all of the patients were treated with anticoagulants and antibiotics (96.15%). 61% were treated with steroids, and 7% with Remdesivir (Fig 1). Despite anticoagulation, every patient had significantly elevated maximum D-dimers that improved slightly throughout infection but remained elevated considerably when last measured. Platelet levels showed a steep downward trend in days leading to death. Oxygen levels fluctuated and did not show a correlation with D-dimers levels (Fig 2). The

most common pulmonary autopsy findings were pneumonia (88.4%), edema (61.5%), Di (50%), and hemorrhage (42%). Acute Diffuse Alveolar Damage (DAD) was seen in only 5 patients, while chronic and organizing DAD and/or pneumonia comprised 65% of all cases. Pulmonary embolism was found in 9 patients (34.62%), and only 2 cases show interstitial lymphocytes. No microvascular microthrombi were identified.

**Table 1. Clinical and autopsy lung findings**

<b>Presentation</b>	
Dyspnea – no. (%)	20 (76.92)
Cough – no. (%)	15 (57.69)
Fever – no. (%)	14 (53.85)
Diarrhea – no. (%)	10 (38.46)
Fatigue or lethargy – no. (%)	9 (34.62)
Myalgia – no. (%)	6 (23.08)
Nausea – no. (%)	6 (23.08)
Altered mental status – no. (%)	6 (23.08)
Anosmia/ageusia – no. (%)	4 (15.38)
Other– no. (%)	5 (19.23)
<b>Mean Length of Hospitalization (range), days</b>	14.92 (0 – 37)
<b>Intubated (%)</b>	24 (92.31)
<b>Comorbidities</b>	
Hypertension – no. (%)	23 (88.46)
Chronic kidney disease* – no. (%)	12 (48.15)
Diabetes mellitus – no. (%)	12 (48.15)
Chronic lung disease <sup>†</sup> – no. (%)	7 (26.92)
Cerebrovascular Accident – no. (%)	6 (23.08)
Obstructive Sleep Apnea – no. (%)	6 (23.08)
Cardiovascular Disease – no. (%)	6 (23.08)
Congestive Heart Failure – no. (%)	5 (19.23)
Other– no. (%)	19 (73.07)
Current Smoker – no. (%)	0
Mean BMI (Range kg/m <sup>2</sup> )	37.71 (19 – 96.9)
Obesity (BMI > 30 kg/m <sup>2</sup> ) – no. (%)	17 (68)
<b>Lung autopsy findings</b>	
<b>Pneumonia – no. (%)</b>	23 (88.46)
Acute – no. (%)	14
Mixed* – no. (%)	8
Organizing – no. (%)	1
<b>ARDS/DAD – no. (%)</b>	13 (50)
Acute – no. (%)	5
Mixed* – no. (%)	8
Organizing – no. (%)	0
<b>Edema – no. (%)</b>	16 (61.54)
<b>Hemorrhage – no. (%)</b>	11 (42.31)
<b>Pulmonary Embolism – no. (%)</b>	9 (34.62)
<b>Type II Pneumocyte Hyperplasia – no. (%)</b>	11 (42.31)
<b>Squamous Metaplasia – no. (%)</b>	11 (42.31)
<b>Megakaryocytes – no. (%)</b>	6 (23.07)
<b>Interstitial lymphocytes</b>	2 (7.69)
<b>Other<sup>†</sup> – no. (%)</b>	13 (50)

Figure 1 - 27

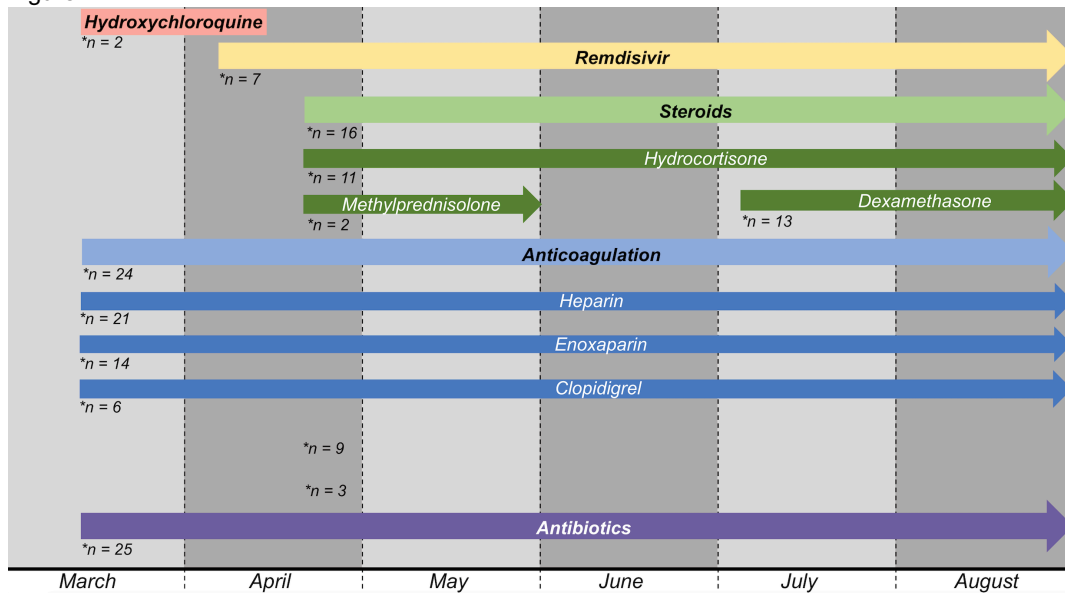
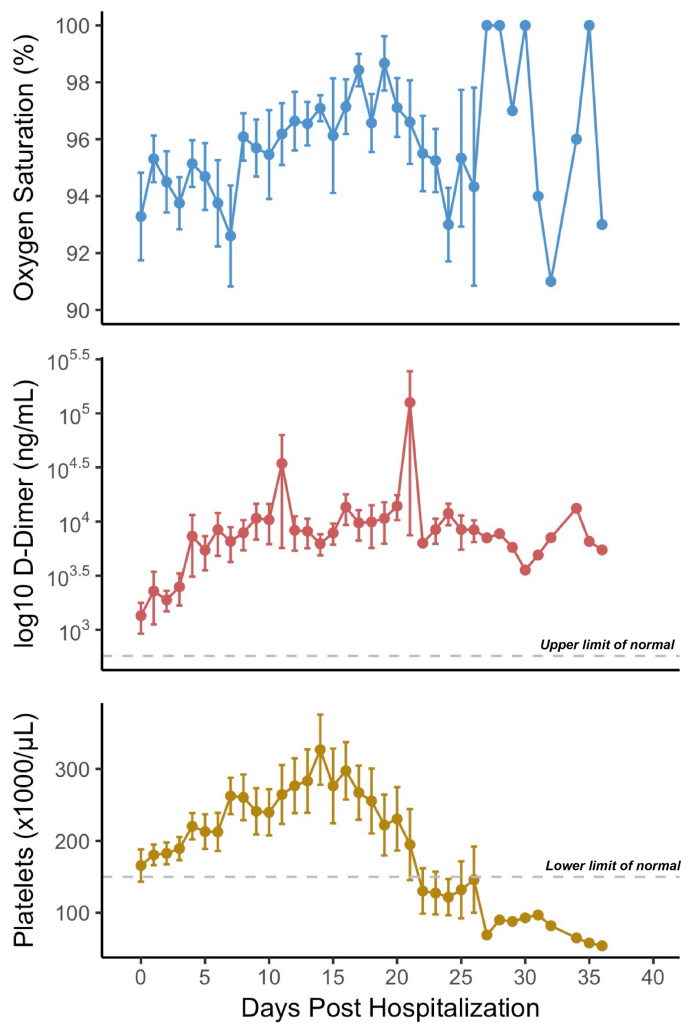


Figure 2 - 27



**Conclusions:** Our study shows that COVID-19 positive patients on ventilator support with prolonged hospitalization die of respiratory failure due to DAD complicated by superimposed, often organizing bronchopneumonia. Despite elevated D-dimers, thromboembolic events are not a predominant finding. While D-dimers stay significantly elevated until the time of death, platelet numbers decline abruptly and do not correlate with the oscillating oxygen levels.

**28 Semi-Automated Death Certificate Error Classification System Characterizes Excessive Death Certificate Error in Code Deaths, Unreflective of Autopsy Completion**

Reiri Sono<sup>1</sup>, Emily Siegel<sup>2</sup>, Zian Tseng<sup>3</sup>, James Salazar<sup>3</sup>

<sup>1</sup>UCSF Pathology, San Francisco, CA, <sup>2</sup>UCSF School of Medicine, San Francisco, CA, <sup>3</sup>University of California, San Francisco (UCSF), San Francisco, CA

**Disclosures:** Reiri Sono: None; Emily Siegel: None; Zian Tseng: None; James Salazar: None

**Background:** The death certificate (DC) is a common source of aggregate mortality data, with its utility limited by substantial classification error. We developed a semi-automated, multiaxial error classification system to evaluate DCs for in-hospital deaths after unsuccessful resuscitation (i.e., code deaths). Since pathophysiological processes surrounding code deaths are often uncertain, we hypothesized that DC error burden is above that of general deaths and autopsied cases have lower DC error burden if updated.

**Design:** We evaluated DCs from consecutive code deaths between 2013-20 at our academic medical center. The classification system, modified from Cambridge et al 2010, consists of 2 axes: Term and Link (**Figure 1**). The Term axis is programmed and applies a dictionary of agonal (e.g., cardiac arrest) and non-specific (e.g., sepsis) terms as adjudicated by 2 physicians (a pathologist and an internist) to classify as unacceptable (U, sole term is agonal), irrelevant information (II, inclusion of agonal terms), and non-specificity (NS, absence of specific terms defined as specific to an organ system, a disease mode such as vascular / infectious / traumatic / neoplastic, and a causative agent if applicable, or else a declaration of uncertainty). The 2 physicians adjudicated the Link axis manually by consensus review of the DC Part 1 causative cascade to classify as incoherent (IC, terms do not form a logical chain of events no matter how repositioned) or incorrectly ordered (IO, forms a chain after repositioning). For autopsied cases, autopsy reports were cross-checked to determine if the DC reflected the final diagnoses.

**Results:** Of 239 death certificates, 148 (62%) had errors; 118 (49%) had a Term error and 74 (31%) had a Link error (**Table 1**). Agonal terms were found in 104 DCs with 4 being Unacceptable. The most frequently used agonal terms were “cardiac arrest” (n=31) and “pulseless electrical activity” (n=11). Nearly 90% of Link errors were not correctable with repositioning (IC). In contrast to the large burden of Link errors, only 16 DCs (7%) included terms with uncertainty spelled out. Autopsied deaths (n=73) had a higher proportion of Term (56% vs 44%, p=0.11) and Link errors (36% vs. 29%, p =0.26), 59% of which did not reflect autopsy diagnoses.

**Table 1:** Number of cases and percentage out of all cases in each error category.

X: Link axis	Incoherent (IC):	Incorrect Ordering (IO):	∅:	Total Cases	
Y: Term axis					
U	N/A	N/A	4 (1.7%)	4 (1.7%)	Term errors: 118 (49.4%)
II+ NS+	6 (2.5%)	2 (0.8%)	13 (5.4%)	21 (8.8%)	
II+ NS-	27 (11.3%)	5 (2.1%)	47 (20.0%)	79 (33.1%)	
II- NS+	3 (1.3%)	1 (0.4%)	10 (4.2%)	14 (5.9%)	
II- NS-	29 (12.3%)	1 (0.4%)	91 (38.1%)*	121 (50.6%)	
Total Cases	65 (27.2%)	9 (3.8%)	165 (69.0%)	239 (100%)	
	Link errors: 74 (31.0%)				

Abbreviations: U, unacceptable; II, Irrelevant Information; NS, Nonspecific; IC, Incoherent; IO, Incorrect Ordering; ∅, no Link error. \* denotes correct filling.

Figure 1 - 28

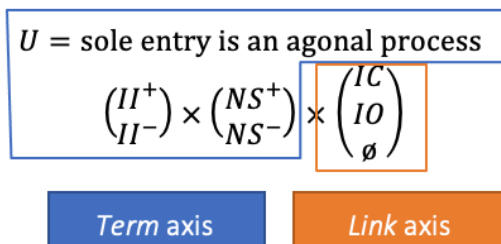


**Figure 1:** full combinations of error types. U (unacceptable); II (Irrelevant Information), having ≥1 agonal term and ≥1 non-agonal term; NS (Nonspecific), missing an etiologically specific term; IC (Incoherent), terms not forming a coherent cascade regardless of rearrangement; IO (Incorrect Ordering), terms forming a coherent cascade after rearrangement; ø = no Link error.

**Conclusions:** Our novel, semi-automated approach identified and characterized substantial (62%) errors in code death DCs compared to the 15-60% published error rates in various settings. We found an especially high burden of agonal terms in place of causative processes perhaps due to the high attention to physiological deficits in code situations. Autopsied cases had more errors, reflecting a failure to update DCs. This study identified a number of areas for quality improvement (e.g., education on acceptability of uncertain terms). Our system provides a framework for an electronically integrated, automated method to mitigate error at the time of DC completion.

## 29 Renal Tubular Epithelial Subnuclear Vacuolization in Hypothermia and Diabetic Ketoacidosis

Burak Tekin<sup>1</sup>, Fabiola Righi<sup>1</sup>, Reade Quinton<sup>1</sup>

<sup>1</sup>Mayo Clinic, Rochester, MN

**Disclosures:** Burak Tekin: None; Fabiola Righi: None; Reade Quinton: None

**Background:** Subnuclear vacuolization of the renal tubular epithelium refers to discrete lipid vacuoles displacing the nuclei towards the lumen. This phenomenon has been associated with a number of conditions sharing fatal ketoacidosis as a common denominator. This retrospective study aimed to investigate renal tubular epithelial subnuclear vacuolization and other postmortem examination findings in fatal hypothermia and diabetic ketoacidosis (DKA) cases.

**Design:** A retrospective search between January 1, 2016 and December 31, 2019 was performed to identify cases for which wording of the primary cause of death included either “hypothermia” or “diabetic ketoacidosis”. For each case, decedent age, sex, comorbidities, toxicology report, vitreous humor analysis, and postmortem examination findings were reviewed. Kidney slides were evaluated for the presence of subnuclear vacuolization of the renal tubular epithelium. Statistical analyses were performed using the Statistical Package for Social Sciences (SPSS) software.

**Results:** Fourteen cases with hypothermia and nineteen cases with DKA were included in the study. Significantly more cases with DKA had focal or diffuse subnuclear vacuolization compared to hypothermia cases (89% vs 43%; *P* = .007). In six cases with DKA, formalin pigment was detected within the subnuclear vacuoles whereas no case with hypothermia had formalin pigment deposition. Comparative analyses of hypothermia and DKA cases revealed further differences: hypothermia cases were older compared to the DKA cases (*P* = .022). Blood ethanol levels were higher in hypothermia cases compared to DKA cases (*P* = .008). More cases with hypothermia had Wischnewsky spots compared to those with DKA (64% vs 11%, *P* = .002).

Statistical analysis of all cases combined revealed that cases with subnuclear vacuolization had higher vitreous creatinine, vitreous beta-hydroxybutyrate, and blood ethanol levels compared to cases without subnuclear vacuolization (*P* = .024, .029, and .023, respectively).

**Conclusions:** The findings corroborate the results of previous studies suggesting a link between increased levels of ketoacidosis and renal tubular epithelial subnuclear vacuolization. As such, this morphologic finding can be seen in different entities, including fatal hypothermia and DKA. Interestingly, formalin pigment deposition localized to the subnuclear vacuoles can be observed in a subset of DKA cases.

### **30 Correlation Between Pupil Diameter and Autopsy Findings: A 20-Year Retrospective Study**

Donald Turbiville<sup>1</sup>, Peter Gershkovich<sup>2</sup>, Vinita Parkash<sup>3</sup>, Declan Mcguone<sup>4</sup>

<sup>1</sup>Yale-New Haven Hospital, New Haven, CT, <sup>2</sup>Yale University School of Medicine, New Haven, CT, <sup>3</sup>Yale School of Medicine, Yale School of Public Health, New Haven, CT, <sup>4</sup>Yale School of Medicine, New Haven, CT

**Disclosures:** Donald Turbiville: None; Peter Gershkovich: None; Vinita Parkash: None; Declan Mcguone: None

**Background:** The CAP 2020 checklist Reporting Protocol for the Examination of Gross Autopsy of Adult Decedents mandates recording bilateral pupil diameter as a required element. The evidence base for this requirement is lacking. In the living, structural and functional pupil evaluation informs on pathologic, pharmacologic and physiologic states. However, functional pupil evaluation is meaningless in decedents, and post-mortem muscle changes (relaxation and rigor) affect pupil diameter. This study aimed to assess the value of pupil diameter as a predictor variable for intracranial and systemic disease at autopsy.

**Design:** Hospital autopsies with recorded pupil diameters between 01/01/2000 to 12/31/2019, identified by keyword search, were reviewed and grouped into 9 cause of death disease categories (ischemic and non-ischemic cardiovascular, malignancy, diabetes, cirrhosis neurologic, autoimmune, mixed/other). Size— difference >1mm (mirroring ophthalmic practice) and more than two standard deviations from the mean—was correlated with age, gender, postmortem interval, brain weight, neuropathologic diagnoses, eye histology (where available), major organ system disease, and cause of death. Two-tailed t-tests were used to compare the means of left and right pupil diameter.

**Results:** 335 pupil diameters were recorded on 171 patients between 2000 and 2019. The mean pupil diameter was 4.4 mm on the right (range 2-10) and 4.3 mm on the left (range 1.5-8). Mean decedent age was 64 yrs (range 0-98 yrs); with a median of 66 yrs. Of 155 patients, with both pupil diameters recorded, 60% had equal and symmetric pupils. Patients with anisocoria had pupil size difference ranging between 1 and 5 mm. 16 patients had pupil diameters greater than two standard deviations of the mean. None of the three groups (All; anisocoria or >2SD size) showed a significant correlation with age, brain weight, post-mortem interval, gender, or category of death. Two cases with intracranial pathology had pupil diameters that exceeded the >2 SD cutoff, both of whom had acute intracranial vascular pathology with mass effect. No correlation with eye pathology was found in 63 cases where ocular exenteration and microscopic examination was performed.

**Conclusions:** Pupil size shows no consistent correlation with quantifiable autopsy findings, although anomalous pupil size (a significantly enlarged pupil) was associated with brain pathology in a small number of cases. Pupil size was also not a reliable predictor of underlying systemic disease or intracranial pathology. Our study suggests that there is limited value, if any, of recording pupil size in autopsy patients, especially considering the lack of standardization of measurement methodology and definitions for pupil size abnormalities in post-mortem patients. A required documentation of this measurement is not supported by our study.



**31 The Utility and Caveats of Ancillary Methods in the Diagnosis of Sars-CoV-2 Infection in Anatomic Pathology Specimens**

Jasmine Vickery<sup>1</sup>, Lindsay Alpert<sup>2</sup>, Aliya Husain<sup>2</sup>, Peter Pytel<sup>3</sup>, John Hart<sup>2</sup>, Jeffrey Mueller<sup>4</sup>, Thomas Krausz<sup>3</sup>, Phillip McMullen<sup>4</sup>

<sup>1</sup>University of Chicago Pritzker School of Medicine, Chicago, IL, <sup>2</sup>University of Chicago, Chicago, IL, <sup>3</sup>University of Chicago Medicine, Chicago, IL, <sup>4</sup>University of Chicago Medical Center, Chicago, IL

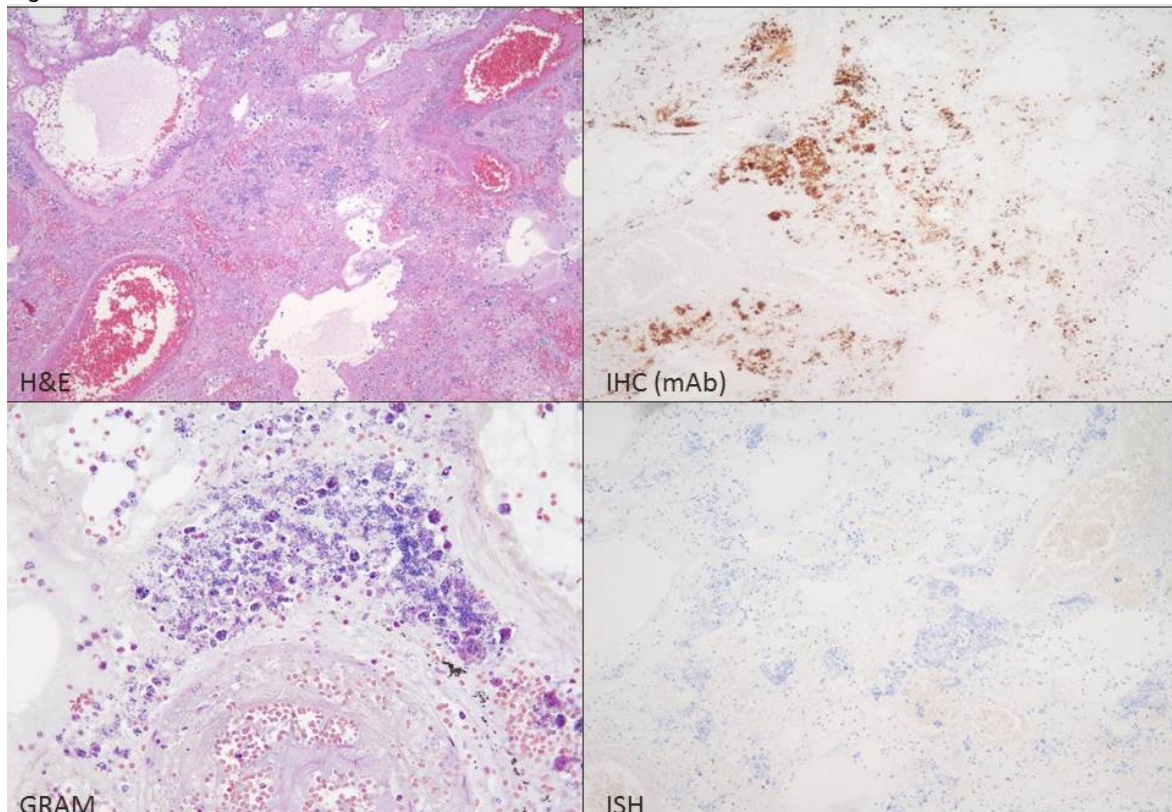
**Disclosures:** Jasmine Vickery: None; Lindsay Alpert: None; Aliya Husain: None; Peter Pytel: None; John Hart: None; Jeffrey Mueller: None; Thomas Krausz: None

**Background:** Immunohistochemical (IHC) and in situ hybridization (ISH) have been used in establishing the diagnosis of severe acute respiratory syndrome coronavirus 2 (SARS-CoV-2) in anatomic pathology specimens. Here we report our experience assessing the utility of these ancillary methods in establishing diagnosis.

**Design:** A positive control (cell block of COVID-19+ Vero Cells) was stained by IHC (Thermo) and an ISH probe (ACD RNAScope). Tissue was obtained from postmortem examinations of 6 SARS-CoV-2 autopsies. Two blinded surveys were performed to assess the utility of IHC in primary diagnosis. In both, a total of ten autopsy lungs (4 from SARS-CoV-2 positive patients and 6 from other infectious and non-infectious pathologies) were stained with the IHC antibody and reviewed by a panel of 6 board-certified pathologists. The cell block control tissue was provided for both surveys, while a portion of COVID+ lung tissue from an autopsy was also included for survey 2.

**Results:** The accuracy and concordance of the examining pathologists in the first survey was 60% and 74% respectively. In the second survey accuracy and concordance increased to 80% and 90% respectively. Only 3 of the 8 total COVID-19 cases were called positive with >50% concordance, representing a sensitivity of only 37.5%. Additionally, two cases of non-COVID lung injury were called positive with >50% concordance, representing a false positivity rate of 16.7%. ISH showed a similar pattern of staining in the assessed cases. Furthermore, ISH was negative in both specimens called positive by IHC.

Figure 1 - 31



**Conclusions:** Ancillary methods may be useful in establishing a diagnosis of COVID-19 infection. The finding of low sensitivity could be attributable to patchy presence of virus across the samples, or simply related to time post-inoculation. False positive staining was due to cross-reactivity of the antibody with multiple species of bacteria. ISH was able to resolve the false-positive cases, and overall recapitulated the staining patterns observed in the positive cases. While our results demonstrate that IHC and ISH can be used to assist in establishing the diagnosis of COVID-19 infection, correlation with the patient's clinical course, pre- and/or post-mortem PCR-based testing may be necessary in some instances.

## **32 Do Not Forget about Dementia! Accuracy and Reliability of the Death Certificate in Reporting Dementia**

Brianna Waller<sup>1</sup>, Thomas Koster<sup>1</sup>, Rachel Martindale<sup>1</sup>, Sharon Mount<sup>1</sup>

<sup>1</sup>University of Vermont Medical Center, Burlington, VT

**Disclosures:** Brianna Waller: None; Rachel Martindale: None; Sharon Mount: None

**Background:** Dementia is a leading cause of death or a contributing factor in the elderly population and ranges from the third to sixth cause of death in those older than 65 years. Documentation of dementia obtained from the death certificate, if accurate and reliable, could be an important source of data to inform public health initiatives. Pathology residents during their autopsy rotation are uniquely qualified to review death certificates and assess accuracy.

**Design:** A retrospective review of all deaths that occurred at an academic teaching hospital in 2018 was performed by pathology residents on their autopsy rotation. Cause and contributory cause of death recorded in the state Electronic Death Registration System (death certification system) were compared to each decedent's electronic medical record (EMR). Patient demographics were recorded using Excel.

**Results:** There were 520 decedents in our cohort. Dementia was listed on the death certificate as either the underlying cause of death or a contributory factor in 33 cases (6.3%). In contrast, 93 (17.5%) of all decedents had a diagnosis of dementia recorded in the EMR and only 35.5% of EMR-documented dementia diagnoses were recorded on their death certificates. For those with a diagnosis of dementia recorded in the EMR, the mean age within this cohort was 81.8 years and there was no sex predilection. Within our dementia cohort, the most common diagnosis subclassification was dementia not otherwise specified (55.9%) followed by Alzheimer's disease (22.6%), vascular dementia (9.7%), Parkinson disease and/or dementia (7.5%), Creutzfeldt-Jakob disease (2.1%), AIDS-related dementia (1.1%), and mixed dementia (1.1%).

**Conclusions:** This review demonstrates that death due to or associated with a dementia diagnosis is often underreported on death certificates and when reported, it is often not sub-classified. Improving the accuracy of death certificate reporting would provide not only a better understanding of the comorbidities associated with dementia, but would also provide invaluable information for the allocation of healthcare resources.